

Acetylcholinesterase inhibitory potential of plant-based phenolics in the treatment of Alzheimer's disease: An *in silico* approach

Mojeed Ayoola Ashiru^{1,2}, Rasheed Adewale Adigun^{2,5}, Musa Oladayo Babalola³, Sherif Olabisi Ogunyemi³, Idris Oladimeji Junaid⁷, Maryam Titilayo Bello-Hassan¹, Mojisola Adebimpe Fategbe⁴, Myah Grace Baker⁶, Kazeem Adelani Alabi², Prince Ozioma Emmanuel¹ & Mohammed O. Balogun⁵

¹ Department of Chemistry and Biochemistry, Texas Tech University, TX 79409-1061, USA

² Department of Chemical Sciences, Fountain University, Osogbo, P.M.B. 4491, Nigeria

³ Department of Biochemistry, University of Lagos, P.M.B. 12003, Nigeria

⁴ Department of Biochemistry, Bowen University, P.M.B. 284, Nigeria

⁵ Biopolymer Modification & Therapeutics Lab, Chemical Cluster, Council for Scientific and Industrial Research, Meiring Naude Road, Brummeria, Pretoria 0001, South Africa

⁶ Department of Animal Nutrition, Texas Tech University, TX 79409, USA

⁷ Department of Chemistry and Chemical Biology, Stevens Institute of Technology, 07030, USA

Corresponding: Mojeed Ayoola Ashiru, Texas Tech University, Lubbock, Texas, USA, Email: mashiru@ttu.edu

Received: June 25, 2025

DOI: 10.14295/bjs.v4i10.769

Accepted: September 24, 2025

URL: <https://doi.org/10.14295/bjs.v4i10.769>

Abstract

Alzheimer's disease is the most prevalent cause of dementia, accounting for more than seventy per cent of all the reported cases. Among the various treatment strategies, inhibiting the action of acetylcholinesterase that breaks down the neurotransmitter acetylcholine is the most common. In this report, thirty-eight phenolic compounds were retrieved from the PubChem database and screened *in silico* against acetylcholinesterase. Non-covalent molecular docking, molecular mechanics-generalized born surface area (MM-GBSA), and molecular dynamics (MD) were used to predict their binding mode, affinity, free energy, and the stability of the protein-ligand complex. These were followed by drug-likeness screening and a rigorous prediction of their absorption, distribution, metabolism, excretion, and toxicity (ADMET) parameters. Myricetin (-13.9 kcal/mol) was predicted to have the highest binding affinity among the phenolics, though lower than the bound donepezil (-16.3 kcal/mol). To increase the binding affinity of myricetin, it was modified via a Schiff base formation, which gave the hydrazine B-1 a binding affinity of -17.7 kcal/mol, higher than that of donepezil. The molecular dynamics simulation showed that the modified ligands have better stability than myricetin. The ADMET and drug-likeness studies showed that the top four phenolics and myricetin analogue derivatives could be further developed as potential drug candidates.

Keywords: acetylcholinesterase, ADMET modeling, Alzheimer's disease, molecular docking, molecular dynamics.

Potencial inibitório da acetilcolinesterase de fenólicos de origem vegetal no tratamento da doença de Alzheimer: Uma abordagem *in silico*

Resumo

A doença de Alzheimer é a causa mais prevalente de demência, correspondendo a mais de setenta por cento de todos os casos relatados. Dentre as diversas estratégias terapêuticas, a inibição da ação da acetilcolinesterase, enzima responsável pela degradação do neurotransmissor acetilcolina, é a mais comum. Neste estudo, trinta e oito compostos fenólicos foram obtidos do banco de dados PubChem e avaliados *in silico* contra a acetilcolinesterase. Utilizaram-se técnicas de docking molecular não covalente, mecânica molecular com área superficial generalizada de Born (MM-GBSA) e dinâmica molecular (MD) para prever o modo de ligação, a afinidade, a energia livre e a estabilidade do complexo proteína-ligante. Em seguida, foram aplicadas análises de

perfil de fármaco (drug-likeness) e uma rigorosa predição dos parâmetros de absorção, distribuição, metabolismo, excreção e toxicidade (ADMET). A miricetina (-13,9 kcal/mol) foi prevista como o composto com maior afinidade de ligação entre os fenólicos, embora inferior ao donepezil ligado (-16,3 kcal/mol). Para aumentar a afinidade de ligação da miricetina, esta foi modificada por meio da formação de uma base de Schiff, originando a hidrazina B-1, com afinidade de ligação de -17,7 kcal/mol, superior à do donepezil. A simulação de dinâmica molecular mostrou que os ligantes modificados apresentaram maior estabilidade em comparação com a miricetina. Os estudos de ADMET e perfil de fármaco indicaram que os quatro principais fenólicos e os derivados análogos da miricetina podem ser futuramente desenvolvidos como potenciais candidatos a fármacos.

Palavras-chave: acetilcolinesterase, modelagem ADMET, doença de Alzheimer, docking molecular, dinâmica molecular.

1. Introduction

Dementia is an age-related condition that affects the cognitive brain processes of memory, language, perception, and cognition, making it challenging to sustain everyday tasks (Jabir; Rehman et al., 2021). Alzheimer's disease (AD) is one of the most well-researched forms of dementia. In the USA, AD is the most prevalent form of dementia, accounting for 60-80 per cent of all cases ("2024 Alzheimer's Disease Facts and Figures," 2024). Alzheimer's disease is projected to affect 12.7 million people aged 65 years and older by 2050 (Association, 2022; Jabir; Shakil et al., 2021).

Protein misfolding and aggregation, oxidative stress, mitochondrial abnormalities, and neuroinflammatory processes are all hallmarks of Alzheimer's disease (AD) at the molecular level (Oliyai et al., 2023). Unfortunately, no definite consensus on the causation of Alzheimer's disease exists, although various hypotheses have been proposed. The most prevalent of them is the cholinergic hypothesis, which postulates that a decrease in the amount of the neurotransmitter acetylcholine (ACh) is associated with cognitive decline. In another amyloid hypothesis, AD has been linked with the formation of β -amyloid ($A\beta$) plaques in the brain (Oh et al., 2022; van Greunen et al., 2017), which is a distinctive feature of AD.

ACh levels in the brain are regulated by the enzyme acetylcholinesterase (AChE, EC number 3.1.1.7), which catalyzes the breakdown of the neurotransmitter ACh. Butyrylcholinesterase (BuChE) also degrades ACh more slowly and to a lesser level (Oh et al., 2022; van Greunen et al., 2017). Interestingly, AChE has also been reported to bind specifically to $A\beta$ and play a crucial role in $A\beta$ plaque formation (van Greunen, Johan van der Westhuizen, et al., 2019).

A single molecule of AChE breaks down over 20,000 molecules of ACh in one second. The enzyme uses three crucial amino acid residues (glutamine, histidine, and serine) known as the catalytic triad at its 20 Å deep gorge. The hydrophobic aromatic residues along the gorge propel ACh into the reaction orientation where the oxygen atom on serine binds to the ACh ester's carbonyl carbon. The loosely-bonded hydrogen atom to the serine gets transferred to the AChE oxygen atom, breaking its intramolecular bond, and thereby releasing choline. Serine containing the remaining acetate gets protonated by a water molecule, leading to the formation of a new bond between the acetate and the oxygen of the water molecule, releasing acetate in the process.

The catalytic triad is restored to its original form, ready to break more ACh (Islam et al., 2019). Therefore, by regulating the clearance of ACh, inhibition of AChE has always been an excellent therapeutic approach. The US Food and Drug Administration (US FDA) has approved three AChE inhibitors for Alzheimer's disease: donepezil, rivastigmine, and galantamine (Tamilselvan et al., 2020). Tacrine was authorized by the FDA but has subsequently been withdrawn owing to hepatotoxicity concerns (Dileep et al., 2022). Despite the numerous treatment options for Alzheimer's disease, interest in plant-based herbal medicine is growing these days due to the lack of complete efficacy and side effects of the approved drugs (Bhandari et al., 2021).

Traditional medicine has been known for using plant-based extracts to treat various diseases, including skin infections, candidiasis, dyspepsia, neurodegenerative disease, cough, and fever (Abuzaid et al., 2020). However, as technology and drug discovery have advanced in the last century, this practice has begun to receive renewed attention (Efferth et al., 2019). The Food and Drug Administration has approved about 25% of new medications, including phytochemicals (Bai et al., 2024; Patridge et al., 2016). Currently, more than USD 65 billion is made annually from the sale of pharmaceuticals derived from plants, with approximately 80% of antibacterial, cardiovascular, immunosuppressive, and anticancer medications being derived from plants (Ramírez-Rendon et al., 2022).

Nevertheless, 6% and 15% of the estimated 450,000 plant species worldwide have undergone pharmacological

and phytochemical screening, respectively (Khan et al., 2023). Thus, many bioactive compounds may have strong physiological effects on several illnesses. For example, antioxidant-rich plants and foods may help reduce Alzheimer's disease by preventing or neutralizing the harmful effects of free radicals (Pritam et al., 2022). An extensive study on the therapeutic benefits of antioxidants in treating Alzheimer's disease has shown promising findings. Gallic acid (GA) and other polyphenols have been demonstrated to enhance cognitive functioning in elderly rats and prevent learning and memory losses following intracerebroventricular (ICV) infusion (Bhuia et al., 2023).

The computational screening approach has recently significantly improved the effectiveness of the present drug development process (Ogunlana, et al., 2023). In the modern day, it is frequently employed to speed up the drawn-out and expensive processes involved in drug discovery and design, from identifying potential targets, typically receptors or enzymes, to creating and refining novel compounds with drug-like properties (Adeoye et al., 2022). Therefore, every computational chemistry technique can influence and expedite a specific stage of the drug discovery process.

These techniques range from quantitative structure-activity relationship (QSAR) to molecular docking, which simulates molecular interaction and generates potent inhibitory ability, or binding affinity (Adeoye et al., 2022). The current study was designed to investigate some phenolic compounds of plant origin and evaluate their inhibitory potential against AChE using molecular docking and molecular dynamics techniques, which may be a possible remedy for neurodegenerative disease.

2. Materials and Methods

2.1 *In silico* studies

Thirty-eight phenolic compounds of plant origin were selected based on their therapeutic properties (Kiokias et al., 2020; Roleira et al., 2015) and then retrieved from the PubChem database (<https://pubchem.ncbi.nlm.nih.gov/>) (Table 1). Their 3D structures were prepared and docked against human acetylcholinesterase (hAChE) protein (PDB ID: 6O4W, resolution: 2.35 Å, wild type) in complex with donepezil to evaluate the phenolic compounds' complementarities and binding affinities. Maestro molecular docking software from the Schrödinger suite (version 12.7) was used for the docking studies.

2.2 Protein preparation

The hAChE (PDB ID: 6O4W) was downloaded from the Protein Data Bank (<https://www.rcsb.org>) and imported into the Maestro workspace. The highly solvated protein was prepared with the protein preparation wizard, keeping most default settings (Madhavi Sastry et al., 2013; Tavella et al., 2022). Considering the importance of water molecules during the acetylcholine hydrolysis (Nemukhin et al., 2013), only the water molecules beyond 3 Å from the het groups were removed during the preprocessing stage, after which all the non-protein het groups were deleted, leaving only the bound donepezil ligand.

The reliability of the binding affinity prediction has been reported to increase when these water molecules cannot form all possible H-bonds, and when they are removed (Pantsar; Poso, 2018). The H-bond was optimized, and the orientations of the water molecules were sampled using PROPKA at pH 7.0 (Rostkowski et al., 2011), followed by the application of restrained minimization using OPLS4 to freely minimize hydrogen atoms while giving room for heavy atom movement within a root mean square deviation (RMSD) of 0.3 Å to relax any strained geometry (Pasala et al., 2019).

2.3 Ligand preparation

The structures of the standard inhibitor donepezil and the 38 phenolic compounds were drawn with Maestro's 2D sketcher, converted to 3D structures upon saving, and subsequently prepared using the LigPrep module from the Maestro software (Schrödinger LigPrep, Schrödinger Release 2021-1, LLC, New York, NY, 2021). The possible ionization states of the compounds were generated using Epik as the pKa predictor at pH 7.0 ± 2.0 (Ashiru et al., 2023). No tautomers were generated from the compounds, and the specified chiralities from the 3D structures were retained. The ligands were subsequently minimized using the OPLS4 force field (Lu et al., 2021).

only the best pose was reported for the output. In addition, post-docking minimisation was also engaged.

Table 1. Phenolic compounds whose 3D structures were docked with acetylcholinesterase (Kiokias et al., 2020; Roleira et al., 2015).

S/N	Name	S/N	Name	S/N	Name	S/N	Name
1	Coumarin	11	<i>p</i> -Hydroxybenzoic acid	21	Naringenin	31	Isorhamnetin
2	Catechin	12	Gallic acid	22	Glycitein	32	Myricetin
3	Gentisic acid	13	Caffeic acid	23	Naringenin chalcone	33	3- <i>o</i> -Caffeoylquinic acid
4	Protocatechuic acid	14	Ferulic acid	24	Genistein	34	Rosmarinic acid
5	<i>p</i> -Coumaric acid	15	Syringic acid	25	Kaempferol	35	Rutin
6	Epicatechin	16	Piperic acid	26	Luteolin	36	4- <i>o</i> -Methyl-epi-gallocatechin
7	Vanillic acid	17	Sinapinic acid	27	Capsaicin	37	Phenyl-6- <i>o</i> -Malonyl-beta-d-glucoside
8	<i>o</i> -Coumaric acid	18	Daidzein	28	Epigallocatechin	38	Epi-gallocatechin-3- <i>o</i> -gallate
9	Eugenol	19	Coumestrol	29	Ellagic acid		
10	Isoeugenol	20	Apigenin	30	Quercetin		

Source: Authors, 2025.

2.4 Receptor grid generation

The 20 Å deep gorge of the hAChE, which contained the bound donepezil crystal, was used to generate the receptor grid for the docking studies using the OPLS4 force field. The grid generation with the excluded cognate ligand (donepezil) allows a confined binding space within the active site for the various ligand poses. The default parameters were kept, like the van der Waals scaling factor of 1.0 and the partial charge cutoff of 0.25. An enclosing box of dimension 10 Å × 10 Å × 10 Å containing the centroid of the donepezil ligand was generated, and this defines the confined space for the docked ligands. No constraint was specified for the interactions of the ligands within the receptor; likewise, no volume was excluded. The catalytic triad at the bottom of the binding gorge consists of Ser200, the protonated glutamic acid Glu202, and His447. Other residues within the Peripheral Anionic Site (PAS) and the Catalytic Anionic Site (CAS) include Tyr72, Trp86, Tyr124, Trp286, and Phe338.

2.5 Non-covalent docking of the phenolic compounds and donepezil against hAChE

The generated receptor grid was retrieved and loaded onto the ligand docking panel, and the prepared ligands were chosen from the project table. The extra precision (XP) scoring function was applied with the ligands docked in flexible states. At the same time, keeping the protein in a "rigid" position. During the docking procedure, the ring conformations and nitrogen inversions were sampled while the Epik state penalty was applied to check if any ligand showed the highest binding affinity in an unfavourable protonation state. With the

XP scoring function, the XP descriptor information was marked to allow the post-visualization of the docking interactions for further rational optimization. No torsional bias sampling was set for any predefined functional group, and nonplanar conformations were not penalized. Different poses per ligand were sampled, but only the best pose was reported for the output. In addition, post-docking minimisation was also engaged.

2.6 MM-GBSA re-docking of the ligands against hAChE

The binding energies of the docked ligands were reassessed according to the combined Molecular Mechanics with Generalized Born and Surface Area (MM-GBSA) scoring function. The docked Post Viewer file from the previous receptor-ligand complex was loaded onto the Prime MM-GBSA panel. The variable-dielectric generalized Born continuum solvation model (VSBG), which uses water as the solvent, was chosen with OPLS4 as the force field. The flexibility of the protein residues within the binding site was changed to cover a distance of 5.0 Å from the ligands. The binding affinities of the ligands were ranked, compared, and analyzed for further rational optimization.

2.7 Molecular dynamic simulations: finding the stability of the protein-ligand complex

The non-covalent docking parameters assume a structural rigidity of the protein with a flexible ligand. On the contrary, the protein and the ligand continually change shape during their interactions. It is, therefore, necessary to check the stability of the protein-ligand complexes. This was done using Desmond's Molecular Dynamics Simulations of the Schrodinger suite. MM-GBSA docked donepezil, myricetin, and the modified myricetin ligands B-1, A-2, and C-3 in complex with hAChE enzyme were used; at the same time, stability was determined by monitoring the potential energy of the system and the root mean square deviation (RMSD) of each protein-ligand complex.

The system for the molecular dynamic simulations was set up using the System Builder in Desmond. The solvation of the complex was achieved using the predefined TIP3P explicit water model within an orthorhombic box using the OPLS4 force field. The required number of sodium and chloride ions was added to neutralize the system, and no volume within the ligand's surroundings was excluded for the salt and ion placements. The built system was simulated for 20 ns while the trajectory was recorded at every 20 ps. The normal temperature and pressure (NPT) ensemble class was chosen at 300 K and 1.01325 bar, respectively, and the model was relaxed before the simulation to minimize the water molecules. The analyses of the various interactions were done using the Simulation Interaction Diagram (SID).

2.8 Analysis of ADME-Tox and drug-likeness

AdmetSAR3 (<https://lmmd.ecust.edu.cn/admetSAR3/>) and SwissADME (<http://www.swissadme.ch/>) were used to perform ligand-based investigations of the selected phytochemicals to identify the molecule that would qualify as a potential hit to reduce viral pathogenesis. The pharmacokinetics and drug-likeness of these compounds were screened using a variety of metrics and guidelines (Adelusi et al., 2022). The drug-likeness parameter was used to predict the route of administration of a drug candidate based on its bioavailability (Rossi et al., 2024). Toxicology risk prediction can show potential adverse effects of phenolic chemicals, facilitating rational medicine design. Predicting the hazardous effects of chemicals, including mutagenic, tumorigenic, irritating, and reproductive impacts, is crucial for drug development from laboratory to clinical application (Rossi et al., 2024).

3. Results

3.1 Reliability of the non-covalent docking procedure

The reliability of the non-covalent docking procedure applied during the in silico studies was validated by re-docking the donepezil ligand into the hAChE enzyme. The conformation with the protonated N-benzylpiperidine moiety with the lowest docking score was the most likely binding mode. The RMSD of the donepezil ligands was calculated and was found to be 0.54 Å, which falls within a 2.0 Å maximum allowed deviation, and therefore the docking procedure was considered valid (Nissink et al., 2002). The results must be presented in the text itself or with the help of Graphs, Figures, and/or Tables.

Considering the superposition using the maximum common structure between the two ligands, the indanone moiety of the ligands was perfectly aligned, and deviation was found within the N-benzylpiperidine rings, with

the chair conformations of the piperidine rings clearly displaying more deviations (Figure 1). As expected, the two bulky groups (the indanone and the phenyl) on the piperidine chair conformation occupied equatorial positions (Adigun et al., 2019). The only difference that caused the deviation was the directions of the indanone and the phenyl groups on the bridging carbons to the piperidine linker.

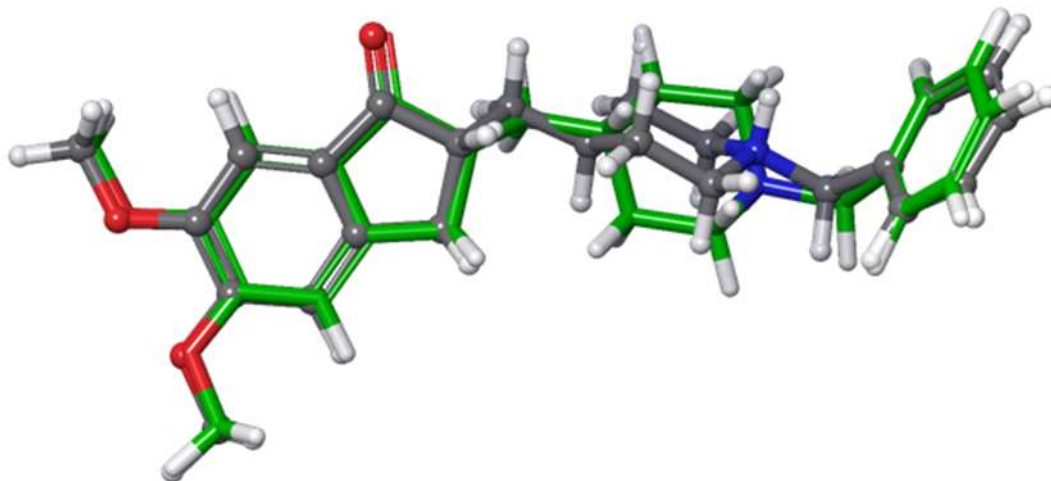


Figure 1. The superposition of re-docked donepezil (grey) and the cognate ligand of the enzyme (green).

3.2 Non-covalent docking of the phenolic compounds and donepezil against hAChE

The binding pose of the co-crystallized donepezil in the active gorge of hAChE enzyme showed the crystal near the catalytic triad, which could be important in preventing acetylcholine from getting in contact with the catalytic Ser203, thereby inhibiting the hydrolysis of acetylcholine (Rants et al., 2022).

Five notable interactions were observed when the 3D molecular interactions of donepezil within the binding pocket of the enzyme were analyzed. The protonated nitrogen of the piperidine ring simultaneously displayed two π -cation interactions with the benzene ring of Tyr337 (distance 4.19 Å) and the pyrrole ring of the CAS residue Trp86 (distance 5.28 Å).

An additional two π - π stacking interactions could be observed between the benzene ring of the N-benzylpiperidine moiety of donepezil and the indole ring of the CAS Trp86 residue; one to the pyrrole ring of the indole backbone (distance 4.36 Å) and the other to the benzene ring (distance 3.72 Å). The carbonyl group of the indanone moiety of donepezil showed a hydrophobically packed hydrogen bond interaction with the nitrogen atom of Phe295 backbone (distance 2.00 Å).

This type of interaction is critical in maintaining ligand stability within the protein's binding pocket. In addition to being a hydrogen bond interaction, the hydrophobic location makes it very difficult to break, thereby maintaining stability during the protein movement. Lastly, the benzene ring of the indanone moiety also showed a π - π stacking interaction with the benzene ring of Trp286 PAS residue (distance 3.81 Å). Most of these interactions are in agreement with earlier reports (Hosseini et al., 2020; van Greunen, van der Westhuizen, et al., 2019). Both the GlideScore (GScore) and the DockScore in kcal/mol for the docked ligands are shown in Table 2.

The docked ionization state with the lowest binding energy was taken as the most probable binding pose and, therefore, was only reported in all the ligands. The observed differences between the GScore and the DockScore were due to Epik state penalties applied to a ligand that shows the lowest binding energy in an unfavourable ionization state. Donepezil showed the lowest binding energy at -16.4 kcal/mol, and many of the docked phenolic ligands displayed comparable energies to donepezil (Table 2). Most binding energy contributions from all the ligands, including donepezil, generally come from their lipophilic interactions.

Table 2. GlideScore (GScore) and the DockScore in kcal/mol for the docked ligands.

S/N	Ligand	Compound CID	XP GScore kcal/mol	DockScore kcal/mol	MMGBSA dG Bind (kcal/mol)
1	Donepezil	(3152)	-16.4	-16.4	-91.4
2	Myricetin	(5281672)	-14.0	-14.0	-75.8
3	Quercetin	(5280343)	-13.5	-13.4	-66.0
4	Epigallocatechin	(72277)	-12.0	-12.0	-55.0
5	Epicatechin	(72276)	-11.7	-11.7	-54.7
6	Catechin	(9064)	-11.7	-11.7	-54.7
7	Luteolin	(5280445)	-11.6	-11.5	-50.8
8	Isorhamnetin	(5281654)	-11.4	-11.4	-58.8
9	Rosmarinic acid	(5281792)	-11.2	-11.2	-54.6
10	Kaempferol	(5280863)	-11.2	-11.2	-56.1
11	Apigenin	(5280443)	-11.0	-11.0	-53.2
12	Naringenin chalcone	(5280960)	-11.4	-10.8	-28.3
13	Rutin	(5280805)	-10.8	-10.7	-64.5
14	Naringenin	(439246)	-10.7	-10.7	-45.3
15	4-o-Methyl epigallocatechin (163184613)		-10.6	-10.6	-67.2
16	Genistein	(5280961)	-11.6	-9.7	-22.6
17	Daidzein	(5281708)	-9.4	-9.4	-51.6
18	Ellagic acid	(5281855)	-9.4	-9.4	-73.5
19	Glycitein	(5317750)	-9.3	-9.3	-61.5
20	Coumestrol	(5281707)	-8.9	-8.9	-53.5
21	3-o-Caffeoylquinic acid	(1794427)	-8.8	-8.8	-26.9
22	Capsaicin	(1548943)	-8.2	-8.2	-61.6
23	Epigallocatechin-3-o-Gallate	(65064)	-8.2	-8.1	-74.9

24	Caffeic acid	(689043)	-7.9	-7.9	-24.9
25	Coumarin	(323)	-7.5	-7.5	-39.1
26	Gallic Acid	(370)	-7.0	-7.0	-23.8
27	<i>o</i> -Coumaric Acid	(637540)	-6.9	-6.9	-24.0
28	Piperic acid	(5370536)	-6.7	-6.7	-40.7
29	Phenyl-6-O-malonyl-beta-D-glucoside (128708)		-6.4	-6.4	-48.5
30	Eugenol	(3314)	-6.4	-6.4	-37.8
31	Sinapinic acid	(637775)	-6.2	-6.2	-24.7
32	Ferulic acid	(445858)	-6.2	-6.2	-23.9
33	Protocatechuic Acid	(72)	-5.9	-5.9	-27.1
34	Isoeugenol	(853433)	-5.8	-5.8	-44.6
35	<i>p</i> -Coumaric Acid	(637542)	-5.4	-5.4	-16.4
36	<i>p</i> -Hydroxybenzoic Acid	(135)	-5.4	-5.4	-11.0
37	Gentisic Acid	(3469)	-5.3	-5.3	-21.9
38	Syringic acid	(10742)	-5.2	-5.2	-17.9
39	Vanillic Acid	(8468)	-5.1	-5.1	-12.4

Source: Authors, 2025.

The binding site contains a lot of lipophilic residues interacting with the lipophilic rings of the ligands. Myricetin, quercetin, epigallocatechin, epicatechin, and catechin showed binding energies of -14.0, -13.5, -12.0, -11.7, and -11.7 kcal/mol, respectively. Interestingly, all of these ligands showed more hydrogen bond interactions than donepezil. This is aided by the presence of several hydroxyl groups on their molecules. Myricetin, for example, has an H-bond pair reward of -5.4 kcal/mol, while donepezil has -1.3 kcal/mol. The 3D interactions of myricetin within the binding gorge revealed two π - π stacking interactions between the benzene ring of Trp286 and the benzene ring of the chromenone moiety (distance 3.99 Å) and the pyranone ring (distance 4.37 Å) (Figure 2).

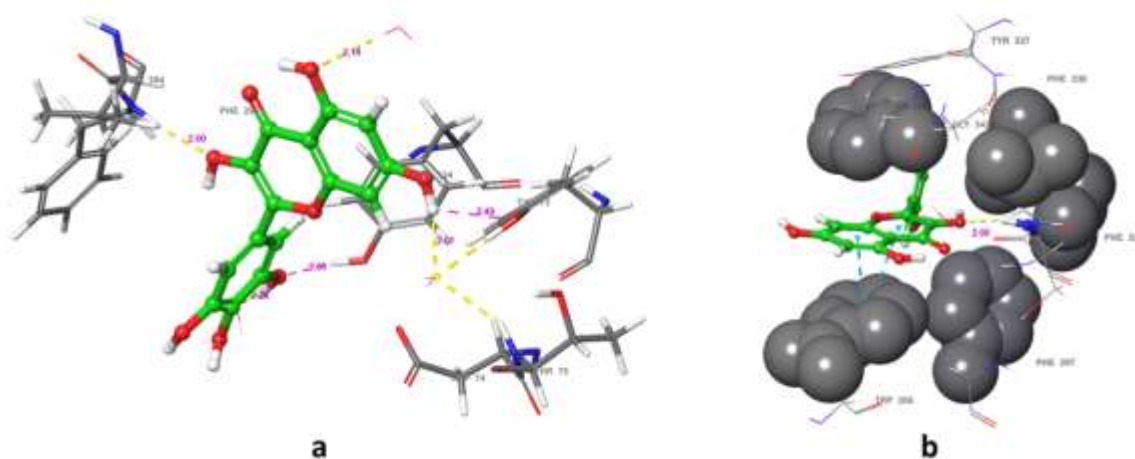


Figure 2. Interactions of myricetin within the binding pocket of hAChE enzyme (PDB ID: 6O4W).

The 7-OH group of the chromenone moiety displayed two water-bridged H-bonds with NH of Tyr75 and the phenolic OH of Tyr72. The NH of Phe295 also showed hydrophobically packed H-bond interaction with the 3-OH group of the chromenone moiety (distance 2.00 Å). As mentioned earlier, this type of H-bond interaction is essential in maintaining ligand stability within the binding pocket. Other interactions within the binding pocket involve H-bond interactions with two water molecules (Figure 3). Due to their structural similarity, myricetin and quercetin had similar binding energies and interactions. In Figure 3, the hydrophobically packed H-bond interaction of myricetin is shown.

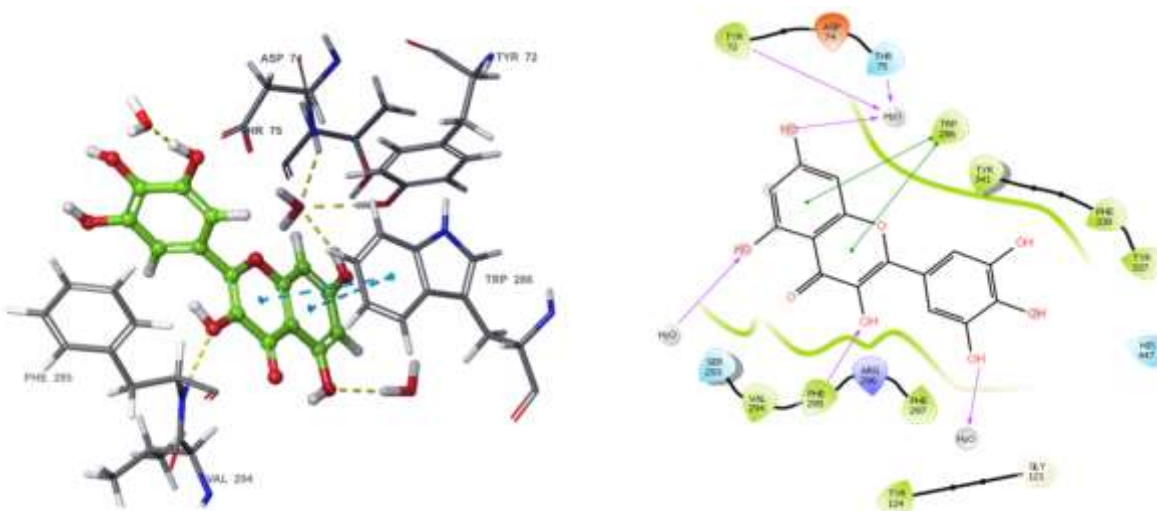


Figure 3. The hydrophobically packed H-bond interaction of myricetin. Source: Authos, 2025.

The binding poses of (a) epigallocatechin, (b) epicatechin, (c) catechin, and (d) luteolin showing non-covalent interactions within the binding site of hAChE enzyme are also shown in (Figure 4).

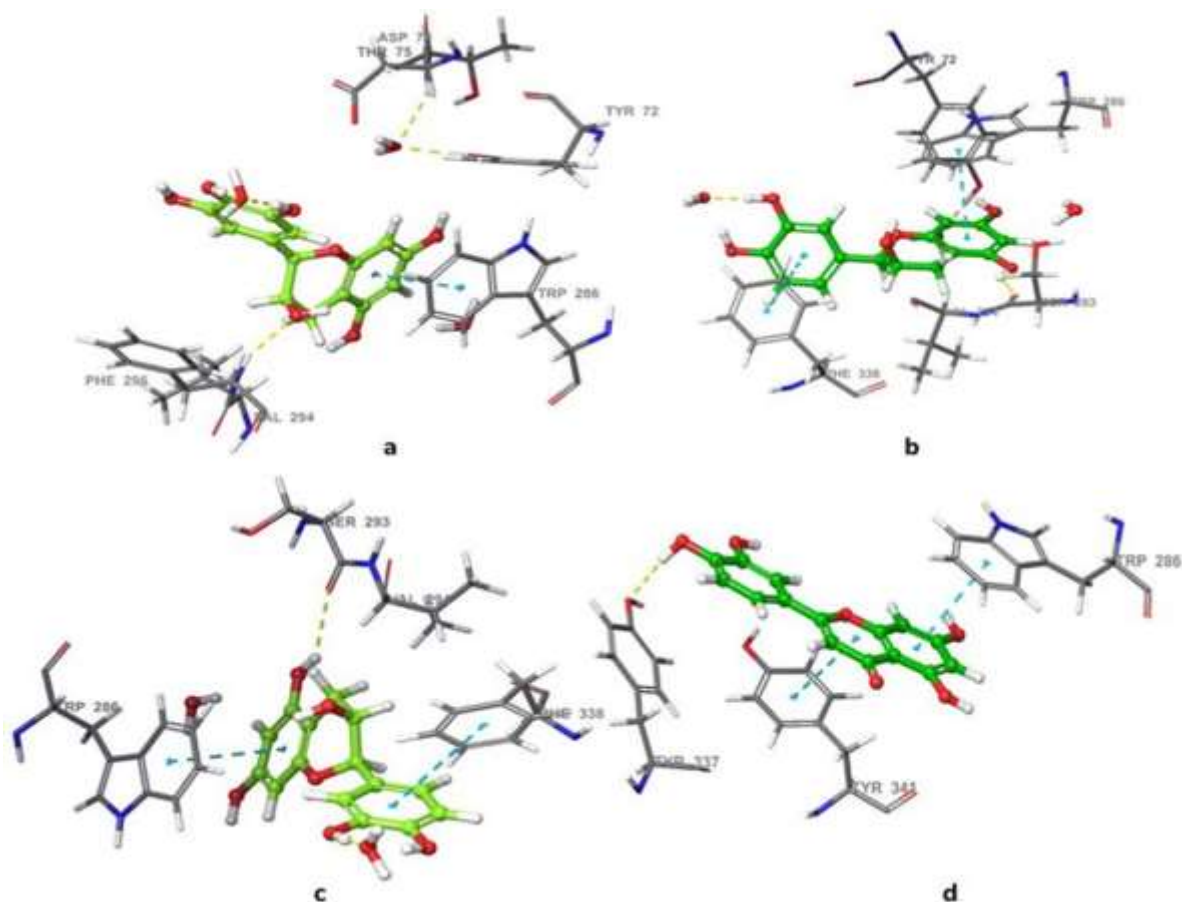


Figure 4. Binding poses of (a) epigallocatechin (b) epicatechin (c) catechin and (d) luteolin showing non-covalent interactions within the binding site of hAChE enzyme (PDB ID: 6O4W). Source: Authors, 2025.

3.3 MM-GBSA-based re-docking of the ligands against hAChE

According to Hubbard and coworkers, better scoring and pose generation functions could be obtained from MM-GBSA than from a non-covalent docking mode (Haider et al., 2011). This is because MM-GBSA gives more accurate results, and its efficiency has been proven in many studies (Genheden; Ryde, 2015; Kaus et al., 2015). As a result, the ligands were docked in MM-GBSA mode to evaluate their binding free energies and poses with the flexibility of the protein residues restricted within 5 Å from the ligand. The result is presented in Table 2 above.

Analysis of the MM-GBSA results shows the preservation of some interactions initially identified by the non-covalent docking. Among these, the π - π stacking interactions between the benzene ring of PAS Trp286 and the benzene ring of the chromenone moiety of myricetin were fully preserved but at a closer distance of 3.71 Å, instead of the original 3.99 Å. Likewise, MM-GBSA indicated H-bond interaction between 3-OH of the pyranone ring and the NH of Phe295 at a distance of 1.96 Å.

One partially preserved interaction is the water-bridged H-bond interaction between 7-OH of the chromenone ring and the OH group of Thr75 side chain instead of the original NH of its amino group.

In addition to the preserved interactions, MM-GBSA identified new vital interactions of myricetin within the binding gorge of hAChE enzyme. The isolated benzene ring of myricetin showed two separate π - π stacking interactions with the benzene rings of Tyr337 and Tyr341 at 5.37 Å and 4.01 Å, respectively. The 7-OH group of the chromenone moiety displayed a water-bridged H-bond interaction with the OH group of Asp74, and the 5'-OH of myricetin's isolated benzene ring showed an H-bond interaction with the phenolic OH of PAS Try124. Other H-bond interactions involved the 5-OH of the chromenone moiety and C=O of Ser293 in a water-bridged interaction, and the C=O of the pyranone moiety showed two H-bond interactions with NH of Arg296 (distance 2.54 Å) and NH of Phe295 (distance 2.58 Å).

Figure 5 shows the superimposed structures of myricetin from the non-covalent docking (green) and the

MM-GBSA (light grey) studies. The positions of the substructures were preserved, but MM-GBSA was able to move the ligand closer to the PAS residues. The high binding affinity shown by myricetin in this study agrees with several previous reports on myricetin's role in treating AD (Gupta et al., 2020; Ramezani et al., 2016; Song et al., 2021a; Wang et al., 2017a).

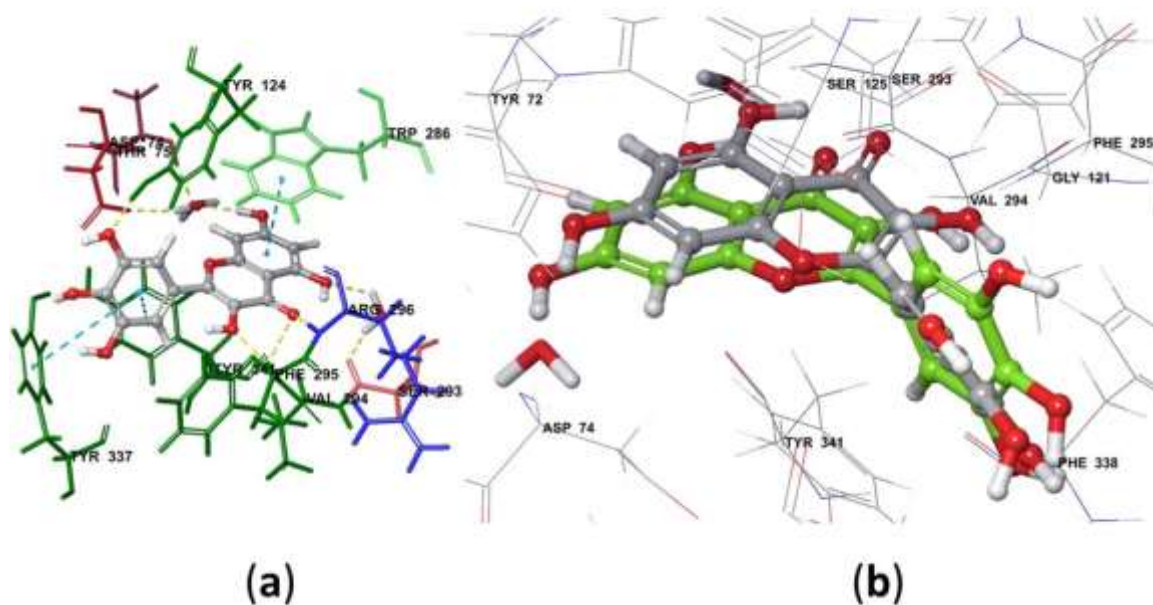
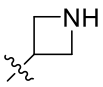
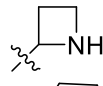
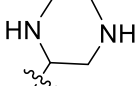
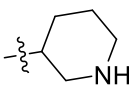
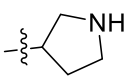


Figure 5. Myricetin (a) re-docked with the MM-GBSA method and the superimposed structures of myricetin (b) from non-covalent docking (green) and MM-GBSA (light grey) within the binding gorge of hAChE (PDB ID: 6O4W). Source: Authors, 2025.

3.4 Structural modification of myricetin for binding affinity optimisation

Myricetin, the ligand with the highest binding affinity, was modified to increase its geometric and electronic complementarities. The chemical modification was done using the carbonyl oxygen of the pyranone ring to form Schiff bases with different amino group-containing compounds. The Custom R-Group Enumeration panel of the Schrödinger suite was used to generate 333 ligands using 38 aliphatic monocyclic rings and 73 aromatic monocyclic rings as R-substituents to give the hydrazides A, the hydrazines B, and the imines C, as shown in (Table 3) and (Figure 6). The ligands were prepared as described previously, and the non-covalent docking was repeated with MM-GBSA analysis. DockScore filtering was applied to enrich the dataset with ligands having a minimum DockScore of -13.9 kcal/mol (using myricetin as the standard). A total of 30 ligands were obtained, and the top 5 ligands are shown in Table 3.

Table 3. The GScore, DockScore, and MM-GBSA values for the top 5 modified myricetins.

Ligand	R	XP GScore kcal/mol	DockScore kcal/mol	MMGBSA dG Bind (kcal/mol)
B-1		-17.7	-17.7	-102.0
A-2		-19.3	-17.7	-84.0
C-3		-18.2	-17.5	-82.4
C-4		-17.1	-16.6	-75.3
B-5		-16.2	-16.2	-91.5

Source: Authors, 2025.

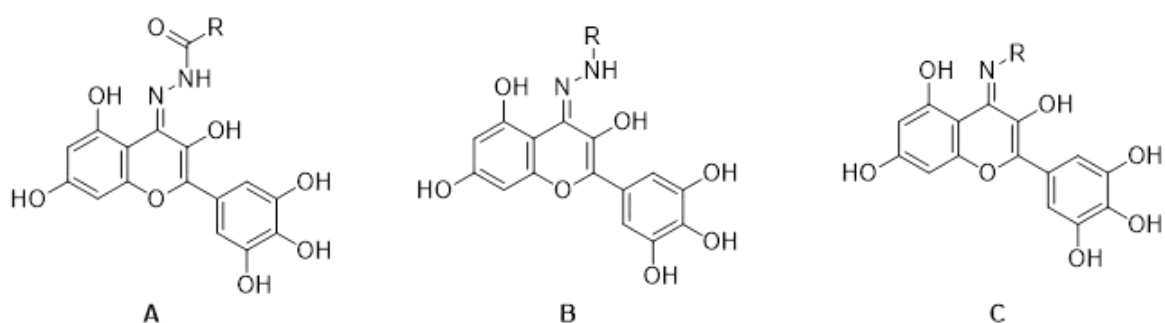


Figure 6. The GScore, DockScore, and MM-GBSA values for the top 5 modified myricetins. Source: Authors, 2025.

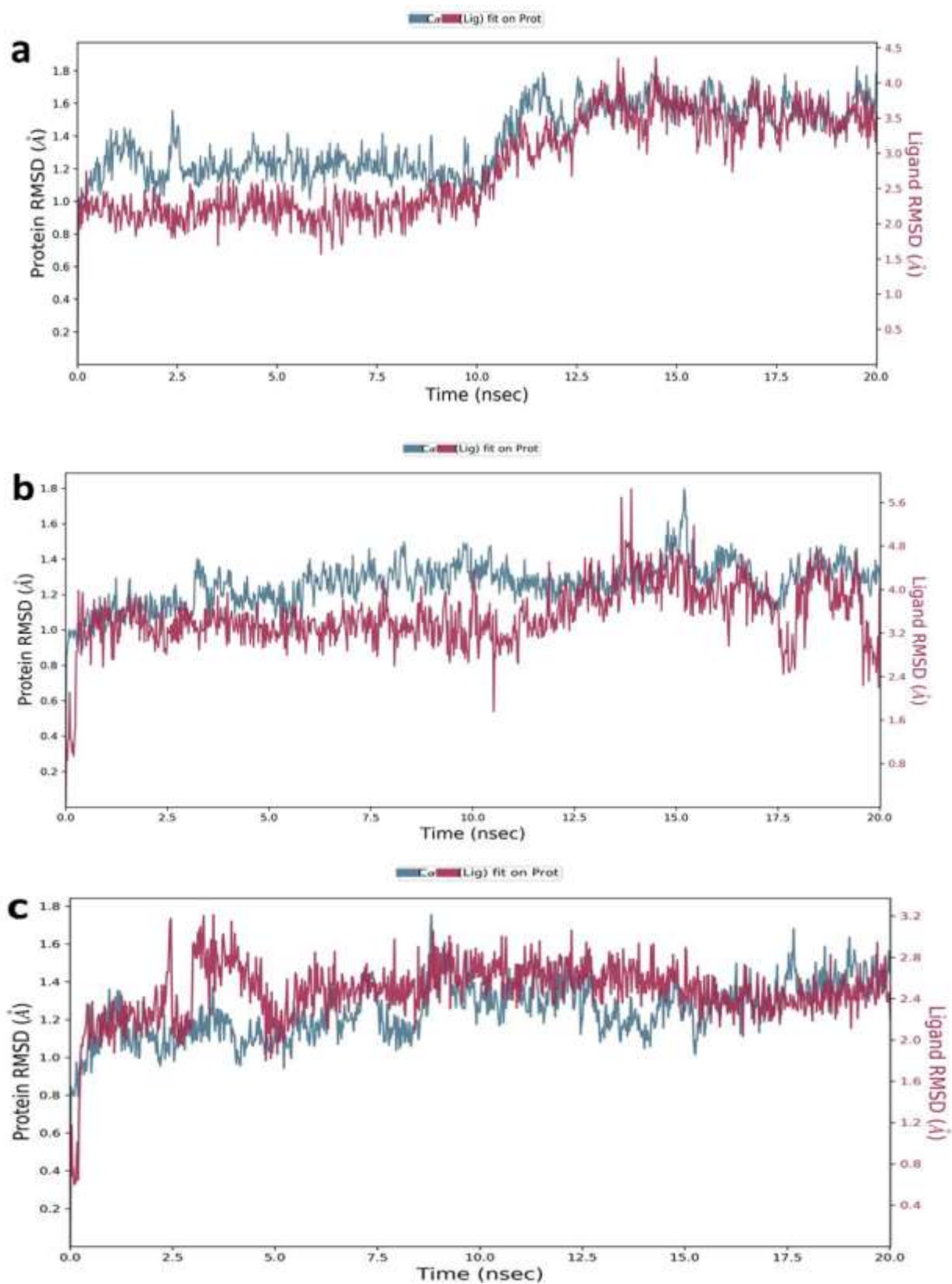
As mentioned earlier, 30 ligands showed higher binding affinities than myricetin after the structural modifications, and from these, ligands B-1, A-2, C-3, and C-4 displayed higher DockScores than donepezil. Using ligand B-1 containing an azetidine substituent as an example, the significant gains over the original myricetin come from lipophilic reward (32%), electrostatic reward (111%), and the electrostatic complementarity for having ligand atoms in a favourable electrostatic environment of the protein (300%). From the frequency of occurrence of the ligands, imine and hydrazine-containing compounds (B and C, respectively) showed better binding affinities than the hydrazide A. This could be due to a reduced interaction from the highly polar hydrazides, as the binding site analysis of the AChE binding gorge showed a highly hydrophobic environment (Barak et al., 2009; Steinberg et al., 1975).

3.5 Molecular dynamics simulations: interaction stability of the protein-ligand complex

The root-mean-square deviation (RMSD) for all the protein-ligand complexes was calculated for every frame in the trajectory. This was done to determine the average displacement of all the atoms for a specific frame compared to a reference frame. The RMSD for frame x is given by:

Where N gives the number of atoms in the atom selection, t is the reference time, and r' is the post-superimposed position of the selected atoms in frame x with respect to the reference frame, while frame x is recorded at time tx.

The procedure is repeated for every frame in the simulation trajectory (Pasala et al., 2019).



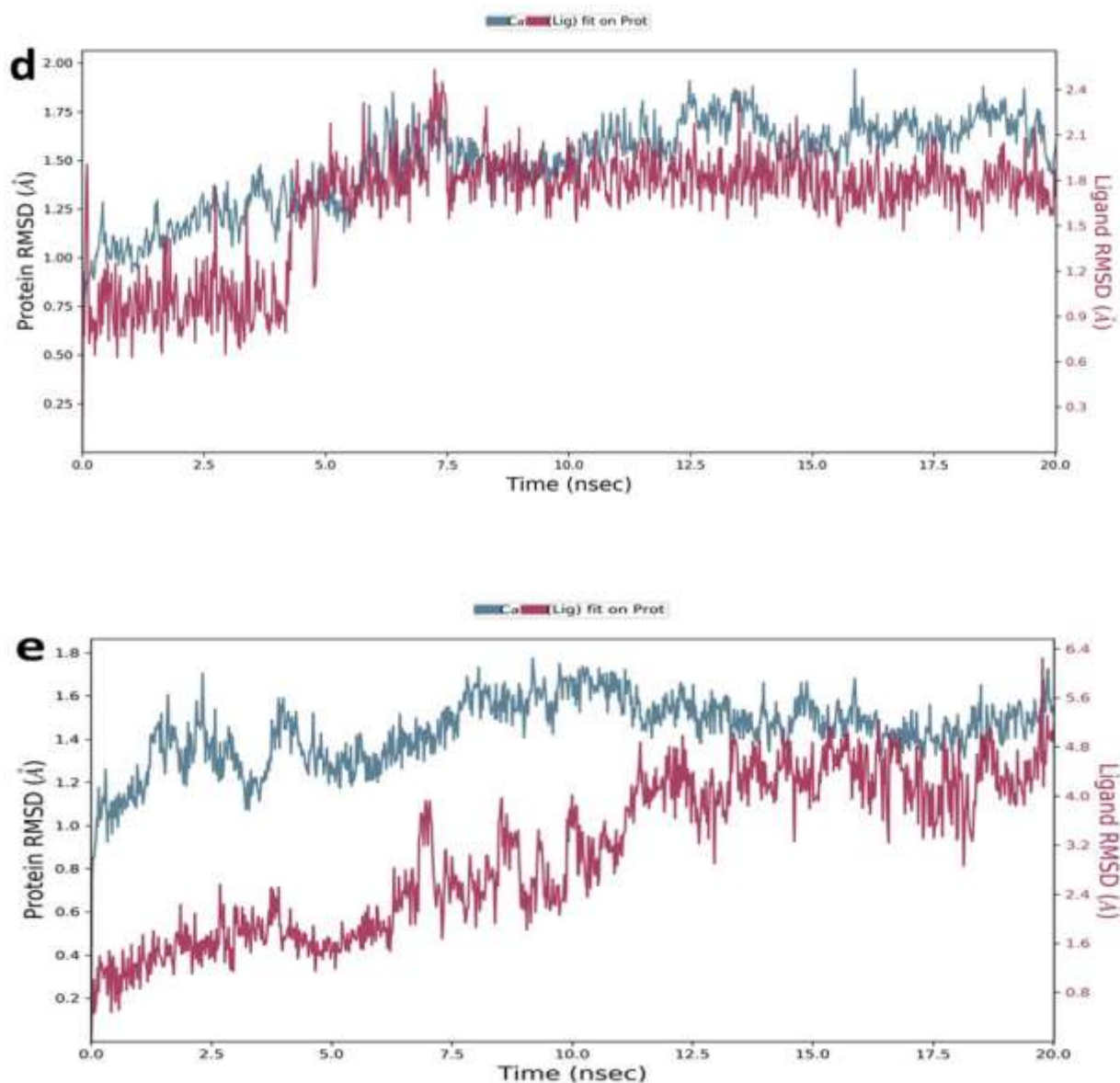


Figure 6. RMSD of ligand (red) and protein C α (blue) for (a) donepezil-AChE, (b) myricetin-AChE, (c) B-1-AChE, (d) A-2-BuChE, and (e) C-3-AChE over 20 ns MD simulation time. Source: Authors, 2025.

The RMSD of the protein-ligand complex for donepezil, myricetin, and modified myricetins B-1, A-2, and C-3 are shown in Figures 6a, b, c, d, and e, respectively. In the donepezil complex, both the protein and the ligand showed equilibration at around 12 ns, and no apparent divergence was observed till the end of the 20 ns simulation time. The protein showed a lower RMSD value than the donepezil ligand, but the fluctuational changes in the two cases were in the order of $\sim 1\text{\AA}$.

Comparing myricetin and its derivatives, the most stable ligand is hydrazine B-1, followed by hydrazide A-2 and then imine C-3, while myricetin showed some levels of divergence towards the end of the simulation. This result agrees with their dock scores and MM-GBSA values. Ligand B-1 achieved the equilibration point at approximately 5 ns, and this was maintained throughout the simulation time. In all the cases, including the donepezil complex, hAChE protein has RMSD values below 1.8\AA while ligands B-1 and A-2 have RMSD values below 3.0\AA and 2.4\AA , respectively, after they attained the equilibration. In contrast, both myricetin and C-3 showed RMSD values above 5\AA .

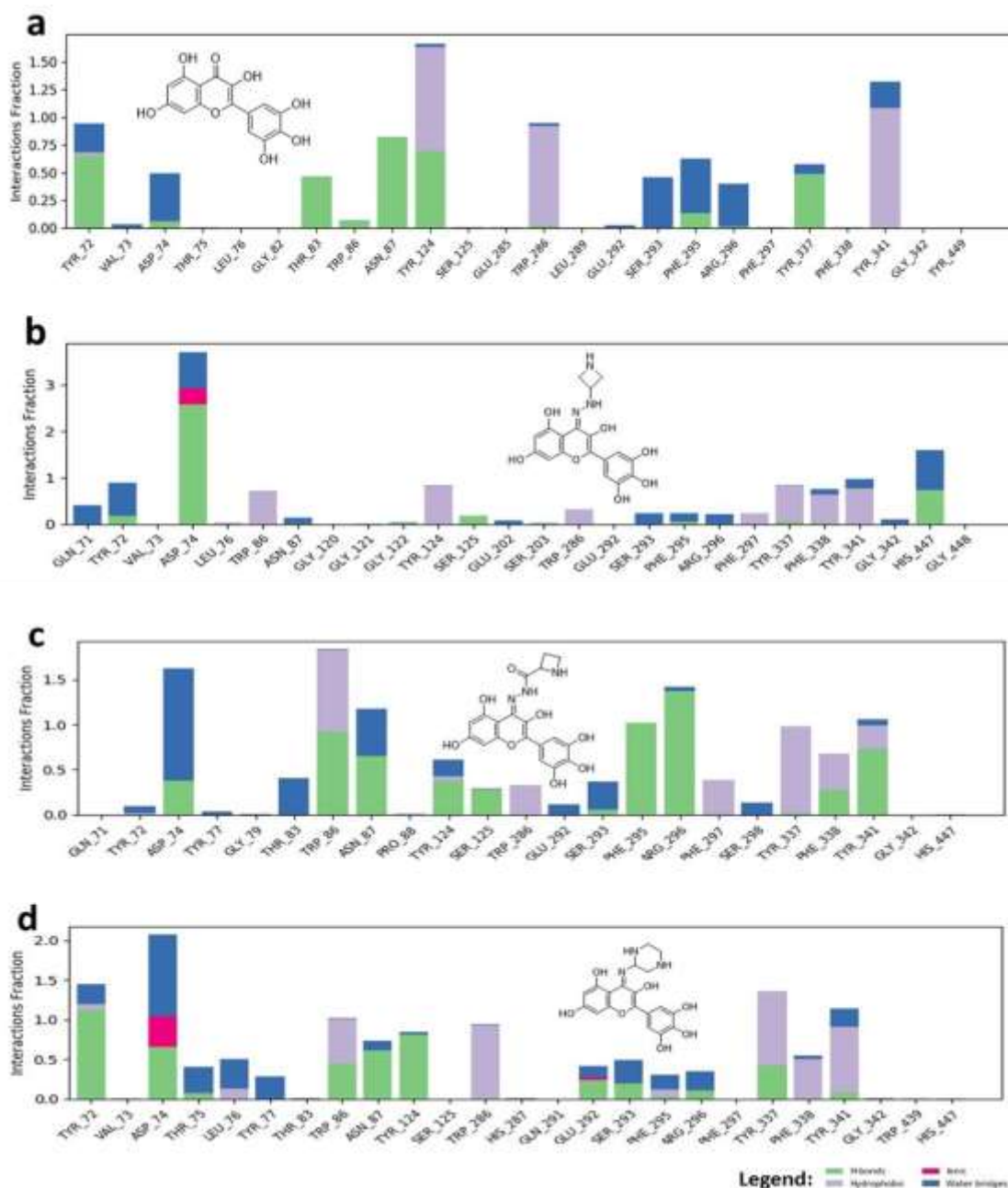


Figure 7. Protein-ligand contacts monitored during a 20 ns MD simulation at 300 K for the (a) hAChE-myricetin complex, (b) AChE-B-1 complex, (c) AChE-A-2 complex, and (d) AChE-C-3 complex. The stacked bar charts of the contacts are normalized to fractions, with values over 1.0 representing protein residues that make multiple contacts with the ligand.

Molecular dynamics studies show the significant binding interactions between donepezil, myricetin, and the myricetin derivatives with the highest MM-GBSA scores. The protein-ligand contacts are shown in Figure 7. As expected, the amino groups of the azetidine substituent on B-1 and A-2 and that of the piperazine substituent on C-3 displayed the most important interactions. Ligand B-1 formed a new water-bridged interaction between Gln71 and its protonated amino group of the azetidine moiety.

At the same time, there was no change in the frequency of interaction with Tyr72 except for the increase in the percentage of water-bridged interaction in B-1 with the accompanying decrease in H-bond interaction compared to myricetin. The interaction of myricetin with Tyr72 was coming from the 5'-OH group of the phenyl moiety at 41% of the simulation time. However, in ligand B-1, the formation of the hydrazine group causes a change in the

binding pose, resulting in a water-bridged interaction between Tyr72 and the protonated amino group of the azetidine group. The significant gain for ligands B-1, A-2, and C-3 came from different interactions with Asp74, with ligand B-1 having the highest interactions with this residue, as shown in the 2D interactions diagram in (Figure 8) (close attention should be paid to the scale of the y-axis).

The interactions include different H-bonds, Pi-cation interactions, and water-bridged H-bond interactions. The interaction of the modified ligands with Thr83 disappeared in B-1 and was almost insignificant in C-3, but was maintained in A-2. All the modified ligands showed an increased frequency of interactions with Trp86. The frequency of interaction with Asn87 only decreased in B-1, saw an increase in A-2, and was maintained in C-3. Additional interactions in the modified myricetins, especially ligands B-1 and A-2, involved Ser125, Glu202, Phe297, Phe338, Gly372, and His447 compared to myricetin. All these could explain the increased DockScore and the stability of the modified ligands.

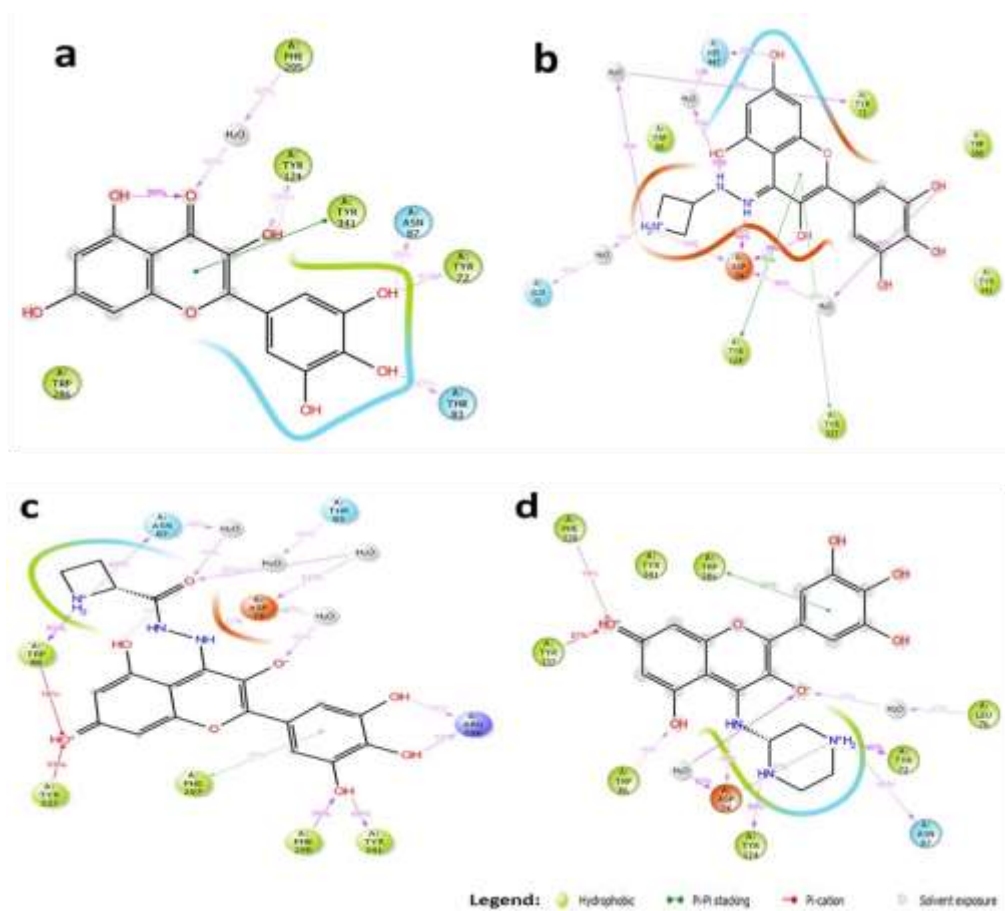


Figure 8. Schematic representation showing the interactions of ligands (a) myricetin, (b) B-1, (c) A-2 and (d) C-3 with the surrounding residues of hAChE during a 20 ns MD simulation at 300 K. Source: Authors, 2025.

3.6 ADME-Tox profiling and drug-likeness

Before a medicine can be approved, it must be screened for pharmacokinetic properties and drug-likeness potential (Ferreira; Andricopulo, 2019). Several guidelines have been proposed to assess if a drug candidate would be orally bioavailable, depending on the pharmacological class. Lipinski's rule is a widely used standard for determining a compound's bioavailability in small-molecule inhibitors (Adelusi et al., 2023). According to Lipinski and colleagues' careful analysis of orally active drugs, a potential drug candidate with an oral route of administration should not violate more than one of the following criteria: molecular weight less than 500 Da; the number of hydrogen bond donors ≤ 5 ; the number of hydrogen bond acceptors ≤ 10 ; and octanol-water partition co-efficient ≤ 5 (Adelusi et al., 2023).

Molecules with poor absorption and low permeability characteristics are considered poor inhibitors, especially if

they violate more than one of these conditions (Adelusi et al., 2022). The results of this investigation, as given in Table 4, suggest that Quercetin and Epicatechin have the potential to be outstanding drug-like molecules since they do not violate any of Lipinski's principles. However, Myricetin and its modified analogues (Table 6) and Epigallocatechin only violated one rule with more than the required number of hydrogen bond donors. As a result, there is a good possibility that any of these compounds may act as promising candidates for drug development.

High-throughput screening tests of several pharmacokinetic parameters are undertaken early in drug development; computational-based ADME-Tox predictions are currently enhancing this labour-intensive and capital-intensive effort. In silico ADME-Tox prediction analyses drug candidates' probable distribution and pharmacokinetics within a single global model. This prediction shows if the candidate will be suitable for drug development in the future, avoiding late-stage attrition and clinical development costs. MetStabOn (Podlewska; Kafel, 2018), admetSAR (Yang et al., 2019), ADMETlab (Xiong et al., 2021), and CypReact (Tian et al., 2018) have all been shown to be highly effective in predicting drug candidates' pharmacokinetic and toxicological endpoints. Early screening for pharmacokinetic and pharmacodynamic features is increasingly being used to prevent undesired qualities from delaying the advancement of a drug candidate into the clinic.

To that end, the top four phenolic compounds and myricetin analogues were subjected to the admetSAR analysis to determine their future potential as drug candidates. Tables 5 and 7 present our results of pharmacokinetic predictions of Quercetin, Myricetin, Epigallocatechin, Epicatechin, the standard drug (donepezil) and myricetin analogues. For the prediction of absorption and distribution features of our drug candidates, we identified human intestinal absorption (HIA), P-glycoprotein substrate, and penetration through the blood-brain barrier (BBB) (Tables 5 and 7).

The selected compounds and myricetin analogues in Tables 5 and 7 depict positive HIA values, including the standard, which may suggest that they are easily absorbed in the gut following ingestion. In the distribution section, Quercetin, Myricetin, Epicatechin, and Epigallocatechin exhibit negative BBB test results, indicating that they cannot cross the blood-brain barrier and thereby protect the central nervous system. However, the standard drug (donepezil) and myricetin analogues have a strong correlation showing a positive score for BBB, indicating that it has a more significant dispersion and may have a neurological impact. Quercetin, Myricetin, Epicatechin, and Epigallocatechin were also predicted to be non-substrates of P-glycoprotein. This implies that these substances may have favourable distribution characteristics. However, the standard drug (donepezil) and the myricetin analogues may act as P-glycoprotein inhibitors, limiting their distribution by P-glycoprotein efflux mediation (Wessler et al., 2013).

The Cyp450 families have been recognised as a key pharmacological parameter in metabolism. Inhibition of these protein families, according to Lynch, may result in drug-drug interactions and bioaccumulation (Kehinde et al., 2022). According to our results, Quercetin and Myricetin inhibit one or more of these metabolic enzymes, while Myricetin analogues exhibit minimal or no inhibition of metabolic enzymes. It is crucial to note that non-acceptable toxicological profiles are important reasons for drugs' failure to pass clinical trials; hence, we have included Ames mutagenicity, acute oral toxicity, hERG inhibition, and carcinogenicity tests in this study (Tables 5 and 7).

The carcinogenicity test results for all compounds, including the myricetin analogues and the standard drug, are negative, which clarifies why they are not carcinogenic. The hERG and Ames mutagenicity are important pharmacological indicators for determining if a drug-like substance is capable of causing cardiac arrhythmia (Babalola et al., 2022) and mutating DNA. The standard drug (donepezil) and Myricetin excel in the Ames mutagenicity test. However, Quercetin, Epigallocatechin, Epicatechin, and Myricetin analogues show positive Ames test results, suggesting they may have the potential to modify DNA. The standard drug (donepezil), which has a positive hERG test result, may influence the heart's potassium channel rhythm (cardiac arrhythmia). In contrast, the other compounds, including myricetin analogues, have negative values for the hERG test.

Table 4. Lipinski's character of donepezil and the top four ligands from the DockScore.

Ligand	Molecular weight	LogP	nHBA	nHBD	nViolation
Donepezil	379.21	3.245	4	0	0
Myricetin	318.04	1.115	8	6	1
Quercetin	302.04	1.448	7	5	0
Epigallocatechin	306.07	0.794	7	6	1
Epicatechin	290.08	1.094	6	5	0

Note: LogP: Octanol-water partition coefficient; nHBD: number of hydrogen bond donors; nHBA: number of hydrogen bond acceptors; nViolation: number of Violation. Source: Authors, 2025.

Table 5. Prediction of the toxicity profiles of donepezil and the top four compounds from the molecular docking.

Parameters/Ligands	Donepezil	Myricetin	Quercetin	Epigallocatechin	Epicatechin
Blood brain barrier (+/-)	+(0.9250)	-(0.7750)	-(0.7750)	-(0.6750)	-(0.6750)
Human intestinal absorption (+/-)	+(0.9838)	+(0.9071)	+(0.9071)	+(0.8922)	+(0.8922)
p-gp inhibitor (+/-)	+(0.8860)	-(0.9166)	-(0.9191)	-(0.9207)	-(0.9411)
LogS (+/-)	-(2.425)	-(2.999)	-(2.999)	-(3.101)	-(3.101)
Human oral Bioavailability (+/-)	-(0.7857)	-(0.5143)	-(0.5429)	-(0.7000)	-(0.7857)
Caco-2	+(0.6843)	-(0.7367)	-(0.6417)	-(0.9372)	-(0.9406)
Carcinogenicity	-(0.9600)	-(1.0000)	-(1.0000)	-(0.9700)	-(0.9700)
Ames mutagenicity	-(0.5800)	-(0.5800)	+(0.8410)	+(0.6100)	+(0.6000)
Acute oral toxicity	III (0.5250)	II (0.7348)	II (0.7348)	IV (0.6433)	IV (0.6433)
Human either - a -go -go inhibition	+(0.9520)	-(0.7812)	-(0.8410)	-(0.4416)	-(0.4678)
Hepatotoxicity	+(0.8677)	+(0.6625)	+(0.9025)	+(0.6427)	-(0.7375)
CYP2C19 Inhibitor (+/-)	-(0.8356)	-(0.9025)	-(0.5823)	-(0.9041)	-(0.9041)
CYP1A2 Inhibitor (+/-)	+(0.5072)	+(0.9106)	+(0.9106)	-(0.9046)	-(0.9046)
CYP3A4 Inhibitor (+/-)	-(0.7411)	+(0.6951)	+(0.6951)	-(0.8309)	-(0.8309)
CYP2C9 Inhibitor (+/-)	-(0.8189)	-(0.5823)	-(0.5823)	-(0.9071)	-(0.9071)
CYP2D6 Inhibitor (+/-)	+(0.8684)	-(0.8553)	-(0.9287)	-(0.9231)	-(0.9231)

Source: Authors, 2025.

Table 6. Lipinski's character of the five modified analogues of Myricetin from the DockScore.

Ligand	Molecular weight	LogP	nHBA	nHBD	nViolation
B-1	371.11	-0.218	9.0	7.0	1
A-2	399.11	0.168	10	7.0	1
C-3	385.13	-0.333	9.0	7.0	1
C-4	384.13	0.327	8.0	6.0	1
B-5	385.13	-0.201	9.0	7.0	1

Note: LogP: Octanol-water partition coefficient; nHBD: number of hydrogen bond donors; nHBA: number of hydrogen bond acceptors; nViolation: number of Violation. Source: Authors, 2025.

Table 7. Prediction of the toxicity profiles of modified analogues of Myricetin from the molecular docking.

Parameters/Ligands	B-1	A-2	C-3	C-4	B-5
Blood brain barrier (+/-)	+(0.0020)	+(0.0000)	+(0.0000)	+(0.0230)	+(0.0020)
Human intestinal absorption (+/-)	+(0.0070)	+(0.0180)	+(0.0750)	+(0.0000)	+(0.0020)
p-gp inhibitor (+/-)	+(0.0000)	+(0.0000)	+(0.0070)	+(0.0020)	+(0.0060)
LogS (+/-)	-(2.5760)	-(2.9420)	-(2.9720)	-(2.6620)	-(2.5480)
Caco-2	-(6.1220)	-(6.1430)	-(6.1360)	-(6.0800)	-(6.1300)
Carcinogenicity	-(0.4860)	-(0.4880)	-(0.1740)	-(0.1460)	-(0.5860)
Ames mutagenicity	+(0.8070)	+(0.8240)	+(0.7540)	+(0.7700)	+(0.8250)
Human either - a -go -go inhibition	-(0.349)	-(0.098)	-(0.249)	-(0.318)	-(0.307)
Hepatotoxicity	+(0.8270)	+(0.7360)	+(0.9030)	+(0.9030)	+(0.8440)
CYP2C19 Inhibitor (+/-)	-(0.0000)	-(0.0000)	-(0.0000)	-(0.0000)	-(0.0000)
CYP1A2 Inhibitor (+/-)	+(0.0060)	-(0.0290)	-(0.6640)	-(0.0680)	-(0.0860)
CYP3A4 Inhibitor (+/-)	-(0.8230)	-(0.9740)	-(0.9580)	+(0.9400)	-(0.9920)
CYP2C9 Inhibitor (+/-)	-(0.0000)	-(0.0070)	-(0.0040)	-(0.0000)	-(0.0010)
CYP2D6 Inhibitor (+/-)	-(0.0000)	-(0.0000)	-(0.0010)	-(0.0000)	-(0.0000)

Source: Authors, 2025.

4. Discussion

The global impact of Alzheimer's disease (AD) constitutes a call for thorough investigation to establish effective and appropriate therapies. Cholinergic neurotransmission (AChE) is importantly implicated in the cognitive deficits of AD and other adult dementias. While treatments aimed at amyloid- β , tau hyperphosphorylation and

immunotherapy have been developed, they were not effective and were discontinued during phase II or III clinical trials (Madav et al., 2019). In the 1970s, a new cholinesterase inhibitor (ChE-I), physostigmine, was developed. The studies suggested that these drugs could produce a small positive effect on symptoms of AD that lasted for a few months and could stabilise/slow the decline in cognition and function during the moderate stages of the disease (Marucci et al., 2021). In 1983, the indanone-derived structurally distinct AChE inhibitor donepezil was synthesised by Sugimoto and coworkers at the Eisai Research Laboratory in Japan (Sugimoto et al., 2002). Donepezil was approved for the treatment of mild to moderate AD as the second drug by the FDA in 1996, and at a higher dose of 23 mg/day, was later approved in 2010 for moderate to severe AD (English, 2012). Donepezil is a potent, specific and reversible AChE inhibitor that exerts its effect in the brain by enhancing acetylcholine concentration in the synaptic cleft (Marucci et al., 2021).

Recently, a worldwide trend has been established for the use of natural products, because they have lower toxicity and are more economical compared with synthetic drugs. In this research, we investigated some phenolic compounds of plant origin and evaluated their inhibitory potential against AChE. To determine the inhibitory role of AChE by a certain phenolic compound, we employed a rigorous series of screening procedures. Molecular docking played a crucial role in this process by allowing the evaluation of both protein–ligand interactions and the binding affinities of the compounds being studied.

Our team docked compounds to AChE, which produced binding energies of -14.0 kcal/mol for Myricetin, -13.5 kcal/mol for quercetin, -12.0 kcal/mol for epigallocatechin, -11.7 kcal/mol for epicatechin and -11.7 kcal/mol for catechin. The reference drug donepezil showed the strongest binding interaction with -16.4 kcal/mol compared to thirty-eight (38) phenolic ligands, which docked onto the protein, even though all these ligands formed more hydrogen bonds than donepezil through the presence of multiple hydroxyl groups on their molecules. All docked ligands, including donepezil, produce their binding energy primarily from lipophilic interactions. The binding site consists of numerous lipophilic residues which bind with the lipophilic rings found in the ligands. Myricetin receives an H-bond pair reward of -5.4 kcal/mol, while donepezil receives -1.3 kcal/mol. The binding gorge of myricetin displayed two π - π stacking interactions between the Trp286 benzene ring and the chromenone moiety benzene ring at 3.99 Å and the pyranone ring at 4.37 Å. The exposed cavity of the target protein requires weak intermolecular forces between ligands and the target protein to maintain energetically favourable ligands (Islam et al., 2025).

We structurally modified the ligand myricetin to enhance its geometric and electronic complementarity with the target protein. The pyranone ring carbonyl oxygen of myricetin underwent Schiff base formation through chemical modification by reacting it with different amino group-containing compounds. The Custom R-Group Enumeration panel in the Schrödinger suite generated 333 ligands by adding 38 aliphatic monocyclic rings and 73 aromatic monocyclic rings as R-substituents to the structure. The reaction produced three product classes: hydrazides (A), hydrazines (B) and imines (C).

The Schrödinger MM-GBSA analysis followed non-covalent docking to assess binding affinities for ligands which were prepared through established protocols. The research produced 30 new ligands, which led to the selection of the top 5 compounds. After structural modifications, the top 5 ligands outperformed myricetin while also showing improved binding affinities compared to donepezil according to DockScore scores. The improved performance of Ligand B-1 resulted from substantial enhancement of lipophilic and electrostatic binding interactions. The AChE binding site appears more compatible with the imine (C) and hydrazine (B) derivatives compared to hydrazides (A), since hydrazides present strong polarity that makes them unsuitable for the hydrophobic AChE binding site.

Molecular docking primarily evaluates the interaction between compounds and the target protein. However, it was also necessary to assess whether the compounds complied with established pharmacokinetic guidelines and to determine their potential toxicity. As shown in the results, Quercetin and Epicatechin exhibited strong potential as drug-like molecules, as they fully comply with Lipinski's rules. In contrast, Myricetin, its modified analogues and Epigallocatechin each violated only one rule, specifically exceeding the recommended number of hydrogen bond donors. As is well established, two or more violations of Lipinski's Rule of Five typically indicate a higher risk of poor bioavailability (Srivastava, 2021). Therefore, these compounds still hold considerable promise as candidates for drug development.

Finally, considering the abundance of hydrogen bonds and their high bioactivity scores, we selected myricetin and its analogues alongside donepezil for molecular simulation analysis. The molecular dynamics simulations showed that all complexes reached stability, with donepezil equilibrating around 12 ns and ligand B-1 around 5 ns. Ligand B-1 was the most stable among the myricetin derivatives, followed by A-2 and C-3, while myricetin

showed instability toward the end. RMSD values confirmed this, with B-1 and A-2 remaining under 3.0 Å and 2.4 Å, respectively, while myricetin and C-3 exceeded 5 Å. These results are consistent with docking and MM-GBSA data, highlighting B-1 as the most promising candidate.

Alzheimer's disease is a complex, progressive, and irreversible neurodegenerative disorder (Simunkova et al., 2019). Iron ions contribute to neuronal damage in AD by promoting oxidative stress (Hofer; Perry, 2016). Myricetin (MYR) is a potent iron chelator that can lower brain iron levels by downregulating transferrin receptor 1 expression, enhancing antioxidant enzyme activity, and decreasing lipid peroxidation. These effects significantly reverse scopolamine-induced cognitive deficits in mice. However, the protective effect of MYR is notably reduced under a high-iron diet (Wang et al., 2017b). Furthermore, since acetylcholinesterase (AChE) plays a key role in learning and memory (Song et al., 2021b), MYR's inhibition of AChE activity adds to its therapeutic potential (Wang et al., 2017b). Overall, these suggest that MYR and its analogue may alleviate neurological and cognitive impairments in AD by modulating brain iron homeostasis and AChE activity. The review by Pluta et al. (2021) also highlighted that myricetin can help reduce learning and memory impairments by inhibiting acetylcholinesterase. Moreover, its anti-inflammatory properties may help prevent acetylcholine depletion caused by inflammatory mediators like IL-1, thereby further supporting cognitive function (Pluta et al., 2021).

The findings presented in this study are derived solely from computational (*in silico*) experiments. Additionally, *in vivo* and *in vitro* laboratory tests are required to validate the outcomes reported here. As this study is predictive, the results should be interpreted with appropriate caution. Also, while we recognise that longer simulations could provide more comprehensive insights, the current analysis provides valuable preliminary insights into the protein-ligand dynamics and interaction stability. Future studies can explore this system further with extended simulations when computational resources become available.

5. Conclusions

In this study, thirty-eight plant-based phenolic compounds were retrieved from the PubChem database. These compounds, in addition to the cognate donepezil, were virtually screened against Acetylcholinesterase. The results of the virtual screening showed that myricetin, quercetin, epigallocatechin, and epicatechin displayed the highest binding affinities, though lower than donepezil. The molecular modification of myricetin was done by Schiff base formation using custom R group enumeration of the Schrödinger suite to give different hydrazides A, hydrazines B, and imines C, which were subsequently subjected to different virtual screenings. Four of these ligands from the three molecular classes showed better binding affinities than donepezil, in addition to the better stability of their protein-ligand complexes.

The result of the molecular dynamics simulation agrees with the docking scores and the MM-GBSA values. From these, various molecular interactions were observed, which include hydrogen bondings, π - π stacking, π -cation, and, more importantly, hydrophobically packed H-bonding, which is essential in maintaining ligand stability within a binding pocket. From the results of the molecular docking, the top four phenolics with the highest binding affinities (myricetin, quercetin, epigallocatechin, and epicatechin), including myricetin analogues derivatives, were subjected to ADMET properties prediction and drug-likeness calculation using the Lipinski rule of five (Ro5).

The favourable predicted results show these compounds could be further developed into potential drug candidates. However, highly powerful phenolic compounds also face hurdles such as poor bioavailability, labile structures, toxicity concerns, and a lack of clinical data. Overcoming these challenges necessitates advanced drug delivery platforms, structural optimisation, uniform formulation, and robust clinical trials. The integration of nanotechnology, artificial intelligence, omics, sustainable production practices, and regulatory support will enable the effective promotion as well as clinical translation of phenolics.

6. Acknowledgements

The authors would like to thank the Centre for High Performance Computing (CHPC, Cape Town, South Africa) for access to the CHPC Lengau Cluster and Schrödinger molecular docking software.

7. Authors' Contributions

Mojeed Ayoola Ashiru and Rasheed Adewale Adigun: Conceptualization, investigation, methodology, validation,

visualization, writing-original draft preparation, writing review, and editing. *Musa Oladayo Babalola, Sherif Olabisi Ogunyemi, Idris Oladimeji Junaid, Maryam Titilayo Bello-Hassan, Mojisola Adebimpe Fategbe*: Conceptualization, writing review, and editing. *Myah Grace Baker, Kazeem Adelani Alabi, Prince Ozioma Emmanuel, and Mohammed O. Balogun*: investigation, validation, visualization, writing-original draft preparation, writing review, and editing.

8. Conflicts of Interest

No conflicts of interest.

9. Ethics Approval

Not applicable.

10. References

- Alzheimer's disease facts and figures. (2024). *Alzheimer's and Dementia*, 20(5), 3708–3821. <https://doi.org/10.1002/alz.13809>
- Abuzaid, H., Amin, E., Moawad, A., Usama Ramadan, Abdelmohsen, Hetta, M., & Mohammed1, R. (2020). Liquid Chromatography High-Resolution Mass Spectrometry Analysis, Phytochemical and Biological Study of Two Aizoaceae Plants: A New Kaempferol Derivative from *Trianthema portulacastrum* L. *Pharmacognosy Research*, 10, 24–30. <https://doi.org/10.4103/pr.pr>
- Adelusi, T. I., Adeyemi, R. O., Ashiru, M. A., Divine, U. C., Boyenle, I. D., Oyedele, A. Q. K., & Adewoye, I. M. (2023). Prediction of Antidiabetic Compounds in *Curcuma longa* – *In vitro* and *In silico* Investigations. *Tropical Journal of Natural Product Research*, 7(10), 4937–4944. <https://doi.org/10.26538/tjnpr/v7i10.33>
- Adelusi, T. I., Oyedele, A. Q. K., Monday, O. E., Boyenle, I. D., Idris, M. O., Ogunlana, A. T., Ayoola, A. M., Fatoki, J. O., Kolawole, O. E., David, K. B., & Olayemi, A. A. (2022). Dietary polyphenols mitigate SARS-CoV-2 main protease (Mpro)–Molecular dynamics, molecular mechanics, and density functional theory investigations. *Journal of Molecular Structure*, 1250, 131879. <https://doi.org/10.1016/j.molstruc.2021.131879>
- Adeoye, M. D., Oyebamiji, A. K., Ashiru, M. A., Adigun, R. A., Olalere, O. H., & Semire, B. (2022). Biological evaluation of selected metronidazole derivatives as anti-nitroreductase via *in silico* approach. *Ecletica Quimica*, 47(4), 27–36. <https://doi.org/10.26850/1678-4618eqj.v47.4.2022.p27-36>
- Adigun, R. A., Malan, F. P., Balogun, M. O., & October, N. (2019). Tetrahydropyrimidinones/thiones stabilized by trifluoromethyl-containing β -diketones. *Journal of Molecular Structure*, 1202, 127281. <https://doi.org/10.1016/j.molstruc.2019.127281>
- Ashiru, M. A., Ogunyemi, S. O., Temionu, O. R., Ajibare, A. C., Cicero-Mfon, N. C., Ihekuna, O. A., Jagun, M. O., Abdulmumin, L., Adisa, Q. K., Asibor, Y. E., Okorie, C. J., Lawal, M. O., Babalola, M. O., Abdulrasaq, I. T., Salau, L. B., Olatunji, I. O., Bankole, M. A., Daud, A. B., & Adeyemi, A. O. (2023). Identification of EGFR inhibitors as potential agents for cancer therapy: pharmacophore-based modeling, molecular docking, and molecular dynamics investigations. *Journal of Molecular Modeling*, 29(5). <https://doi.org/10.1007/s00894-023-05531-6>
- Association, A. (2022). 2022 Alzheimer's disease facts and figures. *Alzheimer's & Dementia*, 18(4), 700-789. <https://doi.org/10.1002/alz.12638>
- Babalola, M. O., Ashiru, M. A., Boyenle, I. D., Atanda, E. O., Oyedele, A.-Q. K., Dimeji, I. Y., Awodele, O., & Imaga, N. A. (2022). In vitro Analysis and Molecular Docking of Gas Chromatography-Mass Spectroscopy Fingerprints of Polyherbal Mixture Reveals Significant Antidiabetic Mixture. *Nigerian Journal of Experimental and Clinical Biosciences*, 10(4), 105-115. https://doi.org/10.4103/njecp.njecp_15_22
- Bai, Y. R., Seng, D. J., Xu, Y., Zhang, Y. D., Zhou, W. J., Jia, Y. Y., Song, J., He, Z. X., Liu, H. M., & Yuan, S. (2024). A comprehensive review of small molecule drugs approved by the FDA in 2023: Advances and prospects. *In European Journal of Medicinal Chemistry*, 276. <https://doi.org/10.1016/j.ejmech.2024.116706>
- Barak, D., Ordentlich, A., Stein, D., Yu, Q., Greig, N. H., & Shafferman, A. (2009). Accommodation of physostigmine and its analogues by acetylcholinesterase is dominated by hydrophobic interactions.

Biochemical Journal, 417(1), 213-222.

- Bhandari, R., Gyawali, S., Aryal, N., Gaire, D., Paudyal, K., Panta, A., Panth, P., Joshi, D. R., Rokaya, R. K., Aryal, P., & Pandey, J. (2021). Evaluation of phytochemical, antioxidant, and memory-enhancing activity of *Garuga pinnata* Roxb. Bark and *Bryophyllum pinnatum* (Lam) Oken. leaves. *The Scientific World Journal*, 2021, 1-7. <https://doi.org/10.1155/2021/6649574>
- Bhuia, M. S., Rahaman, M. M., Islam, T., Bappi, M. H., Sikder, M. I., Hossain, K. N., Akter, F., Al Shamsh Prottay, A., Rokonzaman, M., Güner, E. S., Calina, D., Islam, M. T., & Sharifi-Rad, J. (2023). Neurobiological effects of gallic acid: current perspectives. *In Chinese Medicine (United Kingdom)*, 18(1). <https://doi.org/10.1186/s13020-023-00735-7>
- Dileep, K. V., Ihara, K., Mishima-Tsumagari, C., Kukimoto-Niino, M., Yonemochi, M., Hanada, K., Shirouzu, M., & Zhang, K. Y. J. (2022). Crystal structure of human acetylcholinesterase in complex with tacrine: Implications for drug discovery. *International Journal of Biological Macromolecules*, 210, 172-181. <https://doi.org/10.1016/j.ijbiomac.2022.05.009>
- Efferth, T., Xu, A. L., & Lee, D. Y. W. (2019). Combining the wisdoms of traditional medicine with cutting-edge science and technology at the forefront of medical sciences. *In Phytomedicine*, 64. <https://doi.org/10.1016/j.phymed.2019.153078>
- English, C. (2012). How the FDA forgot the evidence: the case of donepezil 23 mg. *BMJ*, 344. <https://doi.org/10.1136/bmj.e1086>
- Ferreira, L. L. G., & Andricopulo, A. D. (2019). ADMET modeling approaches in drug discovery. *Drug Discovery Today*, 24(5), 1157-1165.
- Genheden, S., & Ryde, U. (2015). The MM/PBSA and MM/GBSA methods to estimate ligand-binding affinities. *Expert Opinion on Drug Discovery*, 10(5), 449-461.
- Gupta, G., Siddiqui, M. A., Khan, M. M., Ajmal, M., Ahsan, R., Rahaman, M. A., Ahmad, M. A., Arshad, M., & Khushtar, M. (2020). Current pharmacological trends on myricetin. *Drug Research*.
- Haider, M. K., Bertrand, H. O., & Hubbard, R. E. (2011). Predicting fragment binding poses using a combined MCSS MM-GBSA approach. *Journal of Chemical Information and Modeling*, 51(5), 1092-1105. <https://doi.org/10.1021/ci100469n>
- Hofer, T., & Perry, G. (2016). Nucleic acid oxidative damage in Alzheimer's disease—explained by the hepcidin-ferroportin neuronal iron overload hypothesis? *In Journal of Trace Elements in Medicine and Biology*, 38, 1-9. <https://doi.org/10.1016/j.jtemb.2016.06.005>
- Hosseini, F., Mohammadi-Khanaposhtani, M., Azizian, H., Ramazani, A., Tehrani, M. B., Nadri, H., Larijani, B., Biglar, M., Adibi, H., & Mahdavi, M. (2020). 4-Oxobenzo[d]1,2,3-triazin-pyridinium-phenylacetamide derivatives as new anti-Alzheimer agents: design, synthesis, in vitro evaluation, molecular modeling, and molecular dynamic study. *Structural Chemistry*, 31(3), 999-1012. <https://doi.org/10.1007/s11224-019-01472-0>
- Islam, B. ul, Jabir, N. R., & Tabrez, S. (2019). The role of mitochondrial defects and oxidative stress in Alzheimer's disease. *In Journal of Drug Targeting*, 27(9), 932-942. <https://doi.org/10.1080/1061186X.2019.1584808>
- Jabir, N. R., Rehman, M. T., Alsolami, K., Shakil, S., Zughaibi, T. A., Alserihi, R. F., Khan, M. S., AlAjmi, M. F., & Tabrez, S. (2021). Concatenation of molecular docking and molecular simulation of BACE-1, γ -secretase targeted ligands: in pursuit of Alzheimer's treatment. *Annals of Medicine*, 53(1), 2332-2344. <https://doi.org/10.1080/07853890.2021.2009124>
- Jabir, N. R., Shakil, S., Tabrez, S., Khan, M. S., Rehman, M. T., & Ahmed, B. A. (2021). In silico screening of glycogen synthase kinase-3 β targeted ligands against acetylcholinesterase and its probable relevance to Alzheimer's disease. *Journal of Biomolecular Structure and Dynamics*, 39(14), 5083-5092. <https://doi.org/10.1080/07391102.2020.1784796>
- Kaus, J. W., Harder, E., Lin, T., Abel, R., McCammon, J. A., & Wang, L. (2015). How to deal with multiple binding poses in alchemical relative protein–ligand binding free energy calculations. *Journal of Chemical Theory and Computation*, 11(6), 2670-2679.
- Kehinde, O. A.-Q., Damilare, B. I., Ogunlana, A., Ayoola, A. M., Opeyemi Emmanuel, A., & Temitope Isaac, A. (2022). Inhibitors of α -glucosidase and angiotensin-converting enzyme in the treatment of type 2 diabetes

- and its complications: A review on *in silico* approach. *Pharmaceutical and Biomedical Research*, 8(4), 237-258. <https://doi.org/10.32598/PBR.8.4.1052.1>
- Khan, S., Hassan, M. I., Shahid, M., & Islam, A. (2023). Nature's toolbox against tau aggregation: An updated review of current research. *In Ageing Research Reviews*, 87. <https://doi.org/10.1016/j.arr.2023.101924>
- Kiokias, S., Proestos, C., & Oreopoulou, V. (2020). Phenolic acids of plant origin-a review on their antioxidant activity in vitro (O/W emulsion systems) along with their in vivo health biochemical properties. *In Foods*, 9(4). <https://doi.org/10.3390/foods9040534>
- Lu, C., Wu, C., Ghoreishi, D., Chen, W., Wang, L., Damm, W., Ross, G. A., Dahlgren, M. K., Russell, E., & Von Bargen, C. D. (2021). OPLS4: Improving force field accuracy on challenging regimes of chemical space. *Journal of Chemical Theory and Computation*.
- Madav, Y., Wairkar, S., & Prabhakar, B. (2019). Recent therapeutic strategies targeting beta amyloid and tauopathies in Alzheimer's disease. *In Brain Research Bulletin*, 146, 171-184. <https://doi.org/10.1016/j.brainresbull.2019.01.004>
- Madhavi Sastry, G., Adzhigirey, M., Day, T., Annabhimoju, R., & Sherman, W. (2013). Protein and ligand preparation: Parameters, protocols, and influence on virtual screening enrichments. *Journal of Computer-Aided Molecular Design*, 27(3), 221-234. <https://doi.org/10.1007/s10822-013-9644-8>
- Marucci, G., Buccioni, M., Ben, D. D., Lambertucci, C., Volpini, R., & Amenta, F. (2021). Efficacy of acetylcholinesterase inhibitors in Alzheimer's disease. *In Neuropsychopharmacology*, 190. <https://doi.org/10.1016/j.neuropharm.2020.108352>
- Nemukhin, A. V., Grigorenko, B. L., Morozov, D. I., Kochetov, M. S., Lushchekina, S. V., & Varfolomeev, S. D. (2013). On quantum mechanical-molecular mechanical (QM/MM) approaches to model hydrolysis of acetylcholine by acetylcholinesterase. *Chemico-Biological Interactions*, 203(1), 51-56.
- Nissink, J. W. M., Murray, C., Hartshorn, M., Verdonk, M. L., Cole, J. C., & Taylor, R. (2002). A new test set for validating predictions of protein-ligand interaction. *Proteins: Structure, Function, and Bioinformatics*, 49(4), 457-471.
- Oh, J. M., Kang, Y., Hwang, J. H., Park, J. H., Shin, W. H., Mun, S. K., Lee, J. U., Yee, S. T., & Kim, H. (2022). Synthesis of 4-substituted benzyl-2-triazole-linked-tryptamine-paeonol derivatives and evaluation of their selective inhibitions against butyrylcholinesterase and monoamine oxidase-B. *International Journal of Biological Macromolecules*, 217, 910-921. <https://doi.org/10.1016/j.ijbiomac.2022.07.178>
- Oliyai, N., Moosavi-Nasab, M., Tanideh, N., & Iraj, A. (2023). Multiple roles of fucoxanthin and astaxanthin against Alzheimer's disease: Their pharmacological potential and therapeutic insights. *In Brain Research Bulletin*, 193, 11-21. <https://doi.org/10.1016/j.brainresbull.2022.11.018>
- Oyedele, A. Q. K., Adelusi, T. I., Ogunlana, A. T., Ayoola, M. A., Adeyemi, R. O., Babalola, M. O., Ayorinde, J. B., Isong, J. A., Ajasa, T. O., & Boyenle, I. D. (2023). Promising disruptors of p53-MDM2 dimerization from some medicinal plant phytochemicals: a molecular modeling study. *Journal of Biomolecular Structure and Dynamics*, 41(12), 5817-5826. <https://doi.org/10.1080/07391102.2022.2097313>
- Oyedele, A. Q. K., Ogunlana, A. T., Boyenle, I. D., Ibrahim, N. O., Gbadebo, I. O., Owolabi, N. A., Ayoola, A. M., Francis, A. C., Eyinade, O. H., & Adelusi, T. I. (2023). Pharmacophoric analogs of sotorasib-entrapped KRAS G12C in its inactive GDP-bound conformation: covalent docking and molecular dynamics investigations. *Molecular Diversity*, 27(4), 1795-1807. <https://doi.org/10.1007/s11030-022-10534-1>
- Pantsar, T., & Poso, A. (2018). Binding affinity via docking: fact and fiction. *Molecules*, 23(8), 1899.
- Pasala, C., Katari, S. K., Nalamolu, R. M., Bitla, A. R., & Amineni, U. (2019). In silico probing exercises, bioactive-conformational and dynamic simulations strategies for designing and promoting selective therapeutics against *Helicobacter pylori* strains. *Journal of Molecular Graphics and Modelling*, 92, 167-179. <https://doi.org/10.1016/j.jmgm.2019.07.015>
- Patridge, E., Gareiss, P., Kinch, M. S., & Hoyer, D. (2016). An analysis of FDA-approved drugs: natural products and their derivatives. *Drug Discovery Today*, 21(2), 204-207.
- Pluta, R., Januszewski, S., & Czuczwar, S. J. (2021). Myricetin as a promising molecule for the treatment of post-ischemic brain neurodegeneration. *In Nutrients*, 13(2), 1-16. <https://doi.org/10.3390/nu13020342>
- Podlewska, S., & Kafel, R. (2018). MetStabOn—online platform for metabolic stability predictions. *International Journal of Molecular Sciences*, 19(4), 1040.

- Pritam, P., Deka, R., Bhardwaj, A., Srivastava, R., Kumar, D., Jha, A. K., Jha, N. K., Villa, C., & Jha, S. K. (2022). Antioxidants in Alzheimer's Disease: Current Therapeutic Significance and Future Prospects. *In Biology*, 11(2). <https://doi.org/10.3390/biology11020212>
- Ramezani, M., Darbandi, N., Khodagholi, F., & Hashemi, A. (2016). Myricetin protects hippocampal CA3 pyramidal neurons and improves learning and memory impairments in rats with Alzheimer's disease. *Neural Regeneration Research*, 11(12), 1976.
- Ramírez-Rendon, D., Passari, A. K., Ruiz-Villafán, B., Rodríguez-Sanoja, R., Sánchez, S., & Demain, A. L. (2022). Impact of novel microbial secondary metabolites on the pharma industry. *In Applied Microbiology and Biotechnology*, 106(5–6), 1855-1878. <https://doi.org/10.1007/s00253-022-11821-5>
- Rants, T. A., Westhuizen, C. J. Van Der, & Zyl, R. L. Van. (2022). Optimization of covalent docking for organophosphates interaction with Anopheles acetylcholinesterase. *Journal of Molecular Graphics and Modelling*, 110, 108054. <https://doi.org/10.1016/j.jmgm.2021.108054>
- Roleira, F. M. F., Tavares-Da-Silva, E. J., Varela, C. L., Costa, S. C., Silva, T., Garrido, J., & Borges, F. (2015). Plant derived and dietary phenolic antioxidants: Anticancer properties. *In Food Chemistry*, 183, 235-258. <https://doi.org/10.1016/j.foodchem.2015.03.039>
- Rossi, A., Stagno, C., Piperno, A., Iraci, N., Panseri, S., Montesi, M., Feizi-Dehnyebi, M., Bassi, G., Di Pietro, M. L., & Micale, N. (2024). Anticancer activity and morphological analysis of Pt (II) complexes: Their DFT approach, docking simulation, and ADME-Tox profiling. *Applied Organometallic Chemistry*. <https://doi.org/10.1002/aoc.7403>
- Rostkowski, M., Olsson, M. H. M., Søndergaard, C. R., & Jensen, J. H. (2011). Graphical analysis of pH-dependent properties of proteins predicted using PROPKA. *BMC Structural Biology*, 11(1), 1-6.
- Schrödinger LigPrep, Schrödinger Release 2021-1, LLC, New York, NY (Schrödinger Release 2021-2). (2021). Schrödinger LLC.
- Simunkova, M., Alwasel, S. H., Alhazza, I. M., Jomova, K., Kollar, V., Rusko, M., & Valko, M. (2019). Management of oxidative stress and other pathologies in Alzheimer's disease. *In Archives of Toxicology*, 93(9), 2491-2513. <https://doi.org/10.1007/s00204-019-02538-y>
- Song, X., Tan, L., Wang, M., Ren, C., Guo, C., Yang, B., Ren, Y., Cao, Z., Li, Y., & Pei, J. (2021a). Myricetin: A review of the most recent research. *Biomedicine & Pharmacotherapy*, 134, 111017.
- Song, X., Tan, L., Wang, M., Ren, C., Guo, C., Yang, B., Ren, Y., Cao, Z., Li, Y., & Pei, J. (2021b). Myricetin: A review of the most recent research. *In Biomedicine and Pharmacotherapy*, 134. <https://doi.org/10.1016/j.biopha.2020.111017>
- Srivastava, R. (2021). Theoretical Studies on the Molecular Properties, Toxicity, and Biological Efficacy of 21 New Chemical Entities. *ACS Omega*, 6(38), 24891-24901. <https://doi.org/10.1021/acsomega.1c03736>
- Steinberg, G. M., Mednick, M. L., Maddox, J., Rice, R., & Cramer, J. (1975). Hydrophobic binding site in acetylcholinesterase. *Journal of Medicinal Chemistry*, 18(11), 1056-1061.
- Sugimoto, H., Ogura, H., Arai, Y., Iimura, Y., & Yamanishi, Y. (2002). REVIEW-New drug and recent technique-research and development of donepezil hydrochloride, a new type of acetylcholinesterase inhibitor. *In Japan Journal of Pharmacology*, 89.
- Tamilselvan, M., Tamilanban, T., & Chitra, V. (2020). Unfolding remedial targets for Alzheimer's disease. *Research Journal of Pharmacy and Technology*, 13(6), 3021-3027.
- Tavella, D., Ouellette, D. R., Garofalo, R., Zhu, K., Xu, J., Oloo, E. O., Negron, C., & Ihnat, P. M. (2022). A novel method for in silico assessment of Methionine oxidation risk in monoclonal antibodies: Improvement over the 2-shell model. *PLoS ONE*, 17. <https://doi.org/10.1371/journal.pone.0279689>
- Tian, S., Jiang, L., Cui, X., Zhang, J., Guo, S., Li, M., Zhang, H., Ren, Y., Gong, G., Zong, M., Liu, F., Chen, Q., & Xu, Y. (2018). Engineering herbicide-resistant watermelon variety through CRISPR/Cas9-mediated base-editing. *Plant Cell Reports*, 37(9), 1353-1356. <https://doi.org/10.1007/s00299-018-2299-0>
- van Greunen, D. G., Cordier, W., Nell, M., van der Westhuyzen, C., Steenkamp, V., Panayides, J., & Riley, D. L. (2017). Targeting Alzheimer's disease by investigating previously unexplored chemical space surrounding the cholinesterase inhibitor donepezil. *European Journal of Medicinal Chemistry*, 127, 671-690. <https://doi.org/10.1016/j.ejmech.2016.10.036>

- van Greunen, D. G., Johan van der Westhuizen, C., Cordier, W., Nell, M., Stander, A., Steenkamp, V., Panayides, J.-L. L., Riley, D. L., van der Westhuizen, C. J., Cordier, W., Nell, M., Stander, A., Steenkamp, V., Panayides, J.-L. L., Riley, D. L., Johan van der Westhuizen, C., Cordier, W., Nell, M., Stander, A., ... Riley, D. L. (2019). Novel N-benzylpiperidine carboxamide derivatives as potential cholinesterase inhibitors for the treatment of Alzheimer's disease. *European Journal of Medicinal Chemistry*, 179, 680-693. <https://doi.org/10.1016/j.ejmech.2019.06.088>
- van Greunen, D. G., van der Westhuizen, C. J., Cordier, W., Nell, M., Stander, A., Steenkamp, V., Panayides, J.-L. L., Riley, D. L., Johan van der Westhuizen, C., Cordier, W., Nell, M., Stander, A., Steenkamp, V., Panayides, J.-L. L., Riley, D. L., van der Westhuizen, C. J., Cordier, W., Nell, M., Stander, A., ... Riley, D. L. (2019). Novel N-benzylpiperidine carboxamide derivatives as potential cholinesterase inhibitors for the treatment of Alzheimer's disease. *European Journal of Medicinal Chemistry*, 179, 680-693. <https://doi.org/10.1016/j.ejmech.2019.06.088>
- Wang, B., Zhong, Y., Gao, C., & Li, J. (2017a). Myricetin ameliorates scopolamine-induced memory impairment in mice via inhibiting acetylcholinesterase and down-regulating brain iron. *Biochemical and Biophysical Research Communications*, 490(2), 336-342.
- Wang, B., Zhong, Y., Gao, C., & Li, J. (2017b). Myricetin ameliorates scopolamine-induced memory impairment in mice via inhibiting acetylcholinesterase and down-regulating brain iron. *Biochemical and Biophysical Research Communications*, 490(2), 336-342. <https://doi.org/10.1016/j.bbrc.2017.06.045>
- Wessler, J. D., Grip, L. T., Mendell, J., & Giugliano, R. P. (2013). The P-glycoprotein transport system and cardiovascular drugs. *Journal of the American College of Cardiology*, 61(25), 2495-2502.
- Xiong, G., Wu, Z., Yi, J., Fu, L., Yang, Z., Hsieh, C., Yin, M., Zeng, X., Wu, C., Lu, A., Chen, X., Hou, T., & Cao, D. (2021). ADMETlab 2.0: An integrated online platform for accurate and comprehensive predictions of ADMET properties. *Nucleic Acids Research*, 49(W1), W5-W14. <https://doi.org/10.1093/nar/gkab255>
- Yang, H., Lou, C., Sun, L., Li, J., Cai, Y., Wang, Z., Li, W., Liu, G., & Tang, Y. (2019). admetSAR 2.0: web-service for prediction and optimization of chemical ADMET properties. *Bioinformatics*, 35(6), 1067-1069.

Funding

Not applicable.

Institutional Review Board Statement

Not applicable.

Informed Consent Statement

Not applicable.

Copyrights

Copyright for this article is retained by the author(s), with first publication rights granted to the journal.

This is an open-access article distributed under the terms and conditions of the Creative Commons Attribution license (<http://creativecommons.org/licenses/by/4.0/>).